Heterogeneous asynchronous time integrators for computational structural dynamics

Anthony Gravouil, Alain Combescure, Michael Brun

Heterogeneous asynchronous time integrators for computational structural dynamics

A. Gravouil[1,2,*,†], A. Combescure[1] and M. Brun[3]

[1]*Université de Lyon, INSA-Lyon, LaMCoS, CNRS UMR 5259, F-69621, Villeurbanne, France*
[2]*Institut Universitaire de France, Paris, France*
[3]*Université de Lyon, INSA-Lyon, LGCIE, EA 4126, F-69621, Villeurbanne, France*

Computational structural dynamics plays an essential role in the simulation of linear and nonlinear systems. Indeed, the characteristics of the time integration procedure have a critical impact on the feasibility of the calculation. In order to go beyond the classical approach (a unique time integrator and a unique timescale), the pioneer approach of Belytschko and co-workers consisted in developing mixed implicit–explicit time integrators for structural dynamics. In a first step, the implementation and stability analyses of partitioned integrators with one time step have been achieved for a large class of time integrators. In a second step, the implementation and stability analyses of partitioned integrators with different time steps were studied in detail for particular cases. However, stability results involving different time steps and different time integrators in different parts of the mesh is still an open question in the general case for structural dynamics. The aim of this paper is to propose a state-of-the art of heterogeneous (different time schemes) asynchronous (different time steps) time integrators (HATI) for computational structural dynamics. Finally, an alternative approach based on energy considerations (with velocity continuity at the interface) is proposed in order to develop a general class of HATI for structural dynamics.

KEY WORDS: structural dynamics; heterogeneous asynchronous time integrators; hybrid multi-time methods; energy-based methods

1. INTRODUCTION

Time integration schemes for linear transient dynamics have been developed for a long time, and it is well established that consistency and stability ensure convergence by h-refinement in time [24]. Both explicit (centered method) and implicit methods (Houblot, Newmark, and Hilber–Hughes–Taylor (HHT)) have been studied and used in great success in a strong link with the finite element method to solve large-scale engineering applications potentially nonlinearly [10, 19, 28, 48]. Even today, the most common time integration methods used in commercial finite element codes were developed by Newmark [3, 20]. In practice, choosing a time integration method depends mainly on stability, accuracy, and target numerical dissipation properties. Indeed, based on Lax's theorem [2], stability and consistency (accuracy) are necessary conditions for the convergence to the exact solution. In this respect, spectral stability is a standard stability metric for linear systems. However, physical energy bounds will be preferred for nonlinear systems [22, 92].

On the one hand, the time discretization of transient dynamics equation consists of checking the following five steps: unconditional stability when applied to linear problems, second-order accuracy, no more than one set of implicit equations that have to be solved for each time step, being

*Correspondence to: A. Gravouil, LaMCoS (Laboratoire de Mécanique des Contacts et des Structures), Bat. J. d'Alembert, 18 rue des Sciences, F-69621 Villeurbanne Cedex, France.
†E-mail: anthony.gravouil@insa-lyon.fr

self-starting, and controllable algorithmic dissipation in the higher-order modes [13, 102]. For instance, popular α-schemes (HHT-α, Wood–Bossak–Zienkiewicz (WBZ)-α, and Chung–Hulbert (CH)-α) allow us to preserve second-order accuracy and numerical dissipation for possible spurious high frequencies [10, 16, 36, 44, 45, 47, 48, 53, 56, 87, 111, 139]; Time Discontinuous Galerkin (TDG), Time eXtended Finite Element Methods (T-XFEM) allow possible temporal discontinuities with high-order accuracy [77, 98, 112, 162]; space–time methods allow space–time refinement and control of accuracy [27, 32, 109, 114, 117]. However, when considering nonlinear problems, the previous implicit schemes can lose their unconditional stability, and many contributions along the years have proposed direct or indirect methods to overcome this difficulty. Indeed, many publications are still devoted to the clarification of specific issues in the nonlinear regime, such as accuracy, stability, energy-decaying properties, overshoot, high-frequency behavior, and numerical integration of internal forces. For that purpose, energy-conserving integrators were proposed by Simo, Laursen, Romero, and others (balance of linear momentum, angular momentum, energy, and energy entropy momentum) [89] [37, 65, 86, 118, 120, 138, 146]; symplectic integrators (Hamiltonian framework with conservative loadings) [40, 85, 147], variational integrators and variational α-schemes [54, 58, 69, 83, 84, 135, 137, 139], and discrete energy-conserving integrators (discrete variational integrators) [85, 119] were also proposed. For instance, a variational symplectic integrator conserves exactly a discrete Lagrangian symplectic structure and has better numerical properties over long integration time, compared with standard integrators. More generally, variational approaches have also been applied to non-smooth contact dynamics [70, 71, 91].

On the other hand, it consists of controlling the time step: choosing a time step depends on the frequency content of the loading, the target accuracy and stability properties of the time integration scheme [1], and also convergence of nonlinear solvers. Adaptive time steps are often needed in order to recover the accuracy and CPU time efficiency [31, 35, 36, 72, 76, 82].

An excellent state of the art on generalized single-step–single-solve (GSSSS) framework algorithms that encompasses the class of linear multi-step methods (LMS) can be found in the works of Tamma *et al.* [98, 133, 135, 137, 139] and Hulbert [102]. GSSSS time integrators can be viewed as the fully discretized time integration framework for the integration of the equation of motion, which inherently contains all previous time integrators (see also [20, 41])).

However, the main drawback of the previous standard approach is in the use of the same time integration scheme (homogeneous time integration) and the same time step for all the finite elements of the mesh (synchronous time integration). This is why an evident improvement consists in developing heterogeneous time integration (each part of the mesh has its own time integration) and asynchronous time integration (each time integration scheme has its own time discretization). Many attempts were carried out on this goal for at least 40 years. Belytschko contributions were central on this topic, and the present paper discusses the state of the art of heterogeneous asynchronous time integration in structural dynamics. The goal of heterogenous asynchronous time integrators (HATI) is to proceed to finite element calculations with different timescales and specific time integrators in each part of the mesh (subdomains) in order to control *locally* the time step and the accuracy (possibility of code coupling). A high ratio between the different timescales (100–1000) can be required. The main difficulty resides in the general property of stability of the HATI (the global stability depends on the stability property of each subdomain and the time gluing on the interface between the subdomains). Engineering applications of HATI can be found for instance in multiphysics, fluid–structure interaction (FSI), multibody dynamics, seismic problems generated by an impact, design of crashworthy automobiles, safety-related impact simulations for aircraft components (localized nonlinearities and fine timescales).

The purpose of this paper is to describe a general methodology to obtain asynchronous coupling methods for different time integration schemes (Newmark, HHT-α, WBZ-α, and CH-α), for instance on the basis of energy considerations. Here, the gluing of subdomains with their own time integrator and their own timescale is ensured with Lagrange multipliers and velocity continuity. Asynchronous kinematic conditions on the interface between the subdomains are obtained by ensuring the zero interface pseudo-energy. Two methods will be derived in this paper. The first method, for which the interface problem involving the Lagrange multipliers is solved at the large timescale, can handle the popular dissipative α-schemes (HHT-α, WBZ-α, and CH-α). In the particular case of Newmark

time integrators, the proposed method matches the PH method proposed by Prakash and Hjelmstad in 2004 [108]. The second method is based on gluing at the micro timescale. It can be viewed as an extension to α-schemes of the GC method proposed by Gravouil and Combescure in 2001 [88, 90].

The present paper is organized as follows. After a brief introduction of the equations of structural dynamics (Section 2), we propose (Section 3) a state of the art of HATI. Then, a specific class of HATI is proposed and applied to a large class of problems in Section 4. Finally, possible extensions and open questions are given in the conclusion.

2. TIME INTEGRATORS FOR STRUCTURAL DYNAMICS

2.1. Equations of structural dynamics

We consider here the finite element method, which conducts to the semi-discretized equilibrium system of Equation (1) for an undamped structure [24]:

$$\begin{aligned} \mathbf{M}\ddot{\mathbf{u}}(t) + \mathbf{f}_{int}(\mathbf{u}(t)) = \mathbf{f}_{ext}(t) \quad \forall t \in [t_0, t_f] \\ \mathbf{u}(t_0) = \mathbf{u}_0,\ \dot{\mathbf{u}}(t_0) = \dot{\mathbf{u}}_0 \end{aligned} \tag{1}$$

where $\mathbf{M}$ is the symmetric definite-positive mass matrix, $\mathbf{u}(t)$ the semi-discretized displacement field at time t, $\mathbf{f}^{int}(\mathbf{u}(t))$ the internal forces at time t (it fulfills the Lipschitz continuity in each time interval), $\mathbf{f}^{ext}(t)$ the given external forces at time t (a smooth function of t is assumed) and possible Dirichlet boundary conditions. In this article, we will no longer consider boundary conditions in space for clarity and simplicity. Single and double superposed dots over a quantity denote respectively its first and second time derivatives. The initial displacement and velocity fields are respectively denoted as $\mathbf{u}_0$ and $\dot{\mathbf{u}}_0$. t_0 and t_f denote respectively the beginning and the end of the time study. Assuming linear elasticity ($\mathbf{f}^{int}(t) = \mathbf{K}\mathbf{u}(t)$ with $\mathbf{K}$ as the global stiffness matrix) involves the following semi-discretized linear transient dynamics equation:

$$\begin{aligned} \mathbf{M}\ddot{\mathbf{u}}(t) + \mathbf{K}\mathbf{u}(t) = \mathbf{f}_{ext}(t) \quad \forall t \in [t_0, t_f] \\ \mathbf{u}(t_0) = \mathbf{u}_0,\ \dot{\mathbf{u}}(t_0) = \dot{\mathbf{u}}_0 \end{aligned} \tag{2}$$

In the previous formalism, equilibrium equation is ensured in a strong sense in time. It is now well established that efficient time integrators are based on weak formulations in time. In other words, prescribing discretized energy balance (or any other kind of discretized balance equations) requires, in a first step, a weak formulation in time of the balance of momentum. As will be shown later, it is a key point for building HATI. As a first step, we can consider the following variational formulation:

$$\mathcal{L}(\mathbf{u}, \dot{\mathbf{u}}) = \mathcal{T}(\dot{\mathbf{u}}) - \mathcal{V}(\mathbf{u}) \tag{3}$$

where the continuous Lagrangian is the difference between the kinetic energy and the potential energy:

$$\begin{aligned} \mathcal{T}(\dot{\mathbf{u}}) &= \frac{1}{2}\dot{\mathbf{u}}^t \mathbf{M}\dot{\mathbf{u}} \\ \mathcal{V}(\mathbf{u}) &= \mathcal{V}_{int} - \mathcal{V}_{ext} = \frac{1}{2}\mathbf{u}^t \mathbf{K}\mathbf{u} - \mathbf{F}_{ext}^t \mathbf{u} \end{aligned} \tag{4}$$

The Euler–Lagrange Equation (2) resulting from this functional can be obtained by the following stationary principle:

$$\begin{aligned} \delta\mathcal{L} = 0 \quad \forall \delta\mathbf{u} \in \mathcal{U}_0\left(H^1(\Omega)\right) \forall t \in [t_0, t_f] \\ \mathbf{u}(t_0) = \mathbf{u}_0,\ \dot{\mathbf{u}}(t_0) = \dot{\mathbf{u}}_0 \end{aligned} \tag{5}$$

Note that we make no attempt to address issues of existence and uniqueness of the solution. In a second step, we can introduce a continuous variational formulation in time based on the following well-known action integral [5, 57]:

$$\mathcal{A}(\mathbf{u}, \dot{\mathbf{u}}) = \int_{t_0}^{t_f} \mathcal{L}(\mathbf{u}, \dot{\mathbf{u}})\ \mathrm{d}t \tag{6}$$

The Euler–Lagrange Equation (2) resulting from this semi-discretized functional can be obtained by a modified stationary principle:

$$\begin{array}{c} \delta\mathcal{A} = 0 \quad \forall \delta\mathbf{u} \in \mathcal{U}_0\left(H^1\left(\Omega,[t_0,t_f]\right)\right), \delta\mathbf{u}\left(.,t_0\right) = \delta\mathbf{u}\left(.,t_f\right) = 0 \\ \mathbf{u}\left(t_0\right) = \mathbf{u}_0,\ \dot{\mathbf{u}}\left(t_0\right) = \dot{\mathbf{u}}_0 \end{array} \tag{7}$$

Indeed, it can easily be shown that it involves the following expression:

$$\delta\mathcal{A} = 0 \Leftrightarrow \int_{t_0}^{t_f} \delta\mathbf{u}^t\left(t\right)\left(\mathbf{M}\ddot{\mathbf{u}}\left(t\right) + \mathbf{K}\mathbf{u}\left(t\right) - \mathbf{f}_{ext}\left(t\right)\right)\,\mathrm{d}t = 0 \tag{8}$$

The semi-discretized weak formulation in time (8) can be considered as a starting point for variational integrators. The time discretization of (8) is also called the *acceleration form* of structural dynamics [102]. However, rather than expressing the inertial effects in terms of acceleration, we can introduce the following Hellinger–Reissner action integral introduced by Washizu [5]:

$$\mathcal{A}_{HR}\left(\mathbf{u},\dot{\mathbf{u}},\mathbf{v}\right) = \int_{t_0}^{t_f} \mathcal{L}_{HR}\left(\mathbf{u},\dot{\mathbf{u}},\mathbf{v}\right)\,\mathrm{d}t \tag{9}$$

where the Hellinger–Reissner Lagrangian is defined as follows:

$$\mathcal{L}_{HR}\left(\mathbf{u},\dot{\mathbf{u}},\mathbf{v}\right) = \mathcal{T}_{HR}\left(\dot{\mathbf{u}},\mathbf{v}\right) - \mathcal{V}\left(\mathbf{u}\right) \tag{10}$$

Here, the velocity $\mathbf{v}$ is a new unknown which is defined by the following modified kinetic energy:

$$\mathcal{T}_{HR}\left(\mathbf{u},\dot{\mathbf{u}},\mathbf{v}\right) = \mathbf{v}^t\mathbf{M}\dot{\mathbf{u}} - \frac{1}{2}\mathbf{v}^t\mathbf{M}\mathbf{v} \tag{11}$$

It involves the following two-field stationary principle:

$$\begin{array}{l} \delta\mathcal{A}_{HR} = 0 \\ \Leftrightarrow \displaystyle\int_{t_0}^{t_f} -\delta\mathbf{u}^t\left(t\right)\left(\mathbf{M}\dot{\mathbf{v}}\left(t\right) + \mathbf{K}\mathbf{u}\left(t\right) - \mathbf{f}_{ext}\left(t\right)\right)\,\mathrm{d}t + \int_{t_0}^{t_f} \delta\mathbf{v}^t\left(t\right)\mathbf{M}\left(\dot{\mathbf{u}}\left(t\right) - \mathbf{v}\left(t\right)\right)\,\mathrm{d}t = 0 \end{array} \tag{12}$$

Then, we obtain the following two Euler–Lagrange equations:

$$\begin{array}{c} \mathbf{M}\dot{\mathbf{v}}\left(t\right) + \mathbf{K}\mathbf{u}\left(t\right) = \mathbf{f}_{ext}\left(t\right) \quad \forall t \in [t_0,t_f] \\ \dot{\mathbf{u}}\left(t\right) - \mathbf{v}\left(t\right) = 0 \quad \forall t \in [t_0,t_f] \\ \mathbf{u}\left(t_0\right) = \mathbf{u}_0,\ \mathbf{v}\left(t_0\right) = \mathbf{v}_0 \end{array} \tag{13}$$

Here, we obtain finally the definition of the velocity $\mathbf{v}$. This first-order system of equation is equivalent to (2). It is also called the *momentum form* of structural dynamics [102]. Its form allows the use of some classes of time integration methods designed for first-order differential equations with the state vector $\mathbf{X} \equiv (\mathbf{u},\mathbf{v})$ (see for instance recent time integrators proposed by Krenk for structural dynamics [111, 118]). It is also the basis for building time integrators for rigid-body dynamics such as the well-known rigid-body energy-momentum-conserving methods [34]. Another interest of the Hellinger–Reissner stationary principle (12) resides in the central role played by the velocity in structural dynamics. Indeed, as very well understood by Washizu, the good duality bracket in structural dynamics is based on the velocity and the linear momentum. In other words, thereafter, kinematic constraints will be introduced on velocity (assuming for instance a linear constraint on the boundary of the domain):

$$\mathbf{L}\dot{\mathbf{u}}\left(t\right) = 0 \tag{14}$$

This can be introduced very easily in a semi-discretized weak formulation in time (either in (6) or (9)) with Lagrange multipliers. Thereafter, we follow the action integral (9). It involves

$$\tilde{\mathcal{A}}\left(\mathbf{u},\dot{\mathbf{u}},\mathbf{v},\boldsymbol{\lambda}\right) = \int_{t_0}^{t_f} \tilde{\mathcal{L}}\left(\mathbf{u},\dot{\mathbf{u}},\mathbf{v},\boldsymbol{\lambda}\right)\,\mathrm{d}t = \int_{t_0}^{t_f} \left(\mathcal{L}_{HR}\left(\mathbf{u},\dot{\mathbf{u}},\mathbf{v}\right) + \boldsymbol{\lambda}^t\left(t\right)\mathbf{L}\dot{\mathbf{u}}\left(t\right)\right)\,\mathrm{d}t \tag{15}$$

where $\boldsymbol{\lambda}$ is the Lagrange multiplier linked to the constraint (14). The corresponding three-field stationary principle is obtained:

$$\begin{aligned}
&\delta\tilde{\mathcal{A}} = 0 \\
&\quad \Leftrightarrow \int_{t_0}^{t_f} -\delta\mathbf{u}^t(t)\left(\mathbf{M}\dot{\mathbf{v}}(t) + \mathbf{K}\mathbf{u}(t) - \mathbf{f}_{ext}(t) - \mathbf{L}^t\Lambda(t)\right) \mathrm{d}t \\
&\qquad + \int_{t_0}^{t_f} \delta\mathbf{v}^t(t)\,\mathbf{M}\left(\dot{\mathbf{u}}(t) - \mathbf{v}(t)\right) \mathrm{d}t \\
&\qquad + \int_{t_0}^{t_f} \delta\boldsymbol{\lambda}^t(t)\,\mathbf{L}\dot{\mathbf{u}}(t)\ \mathrm{d}t = 0
\end{aligned} \tag{16}$$

with the corresponding Euler–Lagrange equations:

$$\begin{aligned}
\mathbf{M}\dot{\mathbf{v}}(t) + \mathbf{K}\mathbf{u}(t) &= \mathbf{f}_{ext}(t) + \mathbf{L}^t\Lambda(t) \quad \forall t \in [t_0, t_f] \\
\dot{\mathbf{u}}(t) - \mathbf{v}(t) &= 0 \quad \forall t \in [t_0, t_f] \\
\mathbf{L}\dot{\mathbf{u}}(t) &= 0 \quad \forall t \in [t_0, t_f] \\
\mathbf{u}(t_0) = \mathbf{u}_0,\ \dot{\mathbf{u}}(t_0) &= \dot{\mathbf{u}}_0
\end{aligned} \tag{17}$$

Here, we obtain the physical meaning of the Lagrange multipliers. $\boldsymbol{\lambda}$ represents the generalized momentum [144], and $\mathbf{L}^t\Lambda$ ($\Lambda = -\dot{\boldsymbol{\lambda}}$) the interface force. In the next part of this paper, the stationary principle (16) will be the basis for a general class of HATI.

Here, we have to notice that (2) and (13) are ODEs in time. However, (17) consists of a differential algebraic equation (DAE). In other words, care has to be taken for the extension of time integrators from ODE to DAE (e.g., [29, 50, 163]). In the following, we will not mention the relation $\dot{\mathbf{u}}(t) - \mathbf{v}(t) = 0$ anymore for clarity.

At this point, we can introduce the time discretization. Let $t_0 < t_1 < \cdots < t_n < t_{n+1} < \cdots < t_f$ be a partition of the time domain, and let $h = t_{n+1} - t_n$ be the time step size. For brevity, a constant h value is assumed hereinafter. Now, following the concept of weak equilibrium in time previously introduced, we assume that the discretized equilibrium equation is only ensured at some times inside h. The corresponding time depends strongly on the considered time integrator. This idea is not new and follows the very powerful approach proposed in the G-α methods [69, 92] or more generally by Tamma *et al.* [133, 137, 139] (see also HHT-α [10], WBZ-α [16], and CH-α [45] for some well-known particular cases of α-schemes). Then, based on the three-field stationary principle (16) and the G-α integrators, we obtain the following discretized/semi-discretized space–time equations:

$$\mathbf{M}\dot{\mathbf{v}}_{n+\xi_g} + \mathbf{K}\mathbf{u}_{n+\xi_f} = \mathbf{f}_{n+\xi_f} + \mathbf{L}^t\boldsymbol{\Lambda}_{n+\xi_f} \quad (\xi_g, \xi_f) \in [0,1]^2 \tag{18}$$

and

$$\int_{t_0}^{t_f} \mathbf{L}\dot{\mathbf{u}}(t)\ \mathrm{d}t = 0 \tag{19}$$

External forces, internal forces, and Lagrange multipliers required by the kinematic constraint are expressed at time $t_{n+\xi_f}$ in (18). As explained by Tamma, a specific parameter is dedicated to acceleration, in order to recover second-order accuracy for the acceleration [139]. Indeed, many well-known second-order-accurate time integrators (for displacement and velocity) can be first-order accurate for acceleration [25, 92, 137, 139]. Then, following Tamma and co-authors, a second-order accuracy for displacement, velocity, and acceleration discretized fields can be recovered through a weak equilibrium in time. Indeed, all designs of algorithms contained within the realm of second-order-accurate LMS possess a specific time level at which a much more rigorous understanding of the acceleration term is obtained [133]. Now, using the two different parame-

Table I. The link between the spectral radius at infinity and the time integrator parameters.

Scheme	α_g	α_f	γ	β
HHT-α	0	$-\alpha_{HHT} = \frac{1-\rho_\infty}{1+\rho_\infty}$	$\frac{1}{2} - \alpha_{HHT}$	$\frac{1}{4}(1-\alpha_{HHT})^2$
WBZ-α	$\alpha_{WBZ} = \frac{\rho_\infty - 1}{1+\rho_\infty}$	0	$\frac{1}{2} - \alpha_{WBZ}$	$\frac{1}{4}(1-\alpha_{WBZ})^2$
CH-α	$\frac{2\rho_\infty - 1}{1+\rho_\infty}$	$\frac{\rho_\infty}{1+\rho_\infty}$	$\frac{3}{2} - 2\alpha_f$	$(1-\alpha_f)^2$

ters ξ_g and ξ_f, the averaged displacements, velocities, accelerations external forces, and Lagrange multipliers read

$$\begin{cases} \dot{\mathbf{v}}_{n+\xi_g} = (1-\xi_g)\dot{\mathbf{v}}_n + \xi_g \dot{\mathbf{v}}_{n+1} \\ \dot{\mathbf{u}}_{n+\xi_f} = (1-\xi_f)\dot{\mathbf{u}}_n + \xi_f \dot{\mathbf{u}}_{n+1} \\ \mathbf{u}_{n+\xi_f} = (1-\xi_f)\mathbf{u}_n + \xi_f \mathbf{u}_{n+1} \\ \mathbf{f}_{n+\xi_f} = (1-\xi_f)\mathbf{f}_n + \xi_f \mathbf{f}_{n+1} \\ \mathbf{\Lambda}_{n+\xi_f} = (1-\xi_f)\mathbf{\Lambda}_n + \xi_f \mathbf{\Lambda}_{n+1} \end{cases} \tag{20}$$

The aim now is to propose a general formalism of modern time integrators with Lagrange multipliers in order to introduce in the next paragraph the HATI. For instance, the classical form for the generalized-α scheme proposed by Chung and Hulbert [45] is characterized by two weighting parameters α_g and α_f. It writes

$$\begin{aligned} &(1-\alpha_g)\mathbf{M}\dot{\mathbf{v}}_{n+1} + \alpha_g \mathbf{M}\dot{\mathbf{v}}_n + (1-\alpha_f)\mathbf{K}\mathbf{u}_{n+1} + \alpha_f \mathbf{K}\mathbf{u}_n \\ &= (1-\alpha_f)\mathbf{f}_{n+1} + (1-\alpha_f)\mathbf{f}_n + \mathbf{L}^t \mathbf{\Lambda}_{n+1-\alpha_f} \end{aligned} \tag{21}$$

From the averaged equilibrium equations in (20) and (21), it can be easily seen that the following relationships between the time integrator parameters hold:

$$\begin{cases} \xi_g = 1 - \alpha_g \\ \xi_f = 1 - \alpha_f \end{cases} \tag{22}$$

In practice, α_g, α_f, γ, and β are fixed in order to achieve unconditional stability, second-order accuracy, and control of spurious high-frequency oscillations while minimizing low-frequency numerical dissipation. Three α-schemes are considered here: HHT-α [10], WBZ-α [16], and CH-α [45]. Furthermore, it is convenient to define the α_g and α_f parameters as a function of the the spectral radius at the high-frequency limit, denoted as ρ_∞, characterizing the amount of numerical dissipative energy in the high-frequency range. The two other algorithmic parameters γ and β involved in the classical Newmark formulae [3] are then expressed in terms of α_g and α_f as has been resumed in Table I. From Equation (20), the averaged acceleration, velocity, and displacement can be put in the following form:

$$\begin{cases} \dot{\mathbf{v}}_{n+\xi_g} = \dot{\mathbf{v}}_n + \xi_g \Delta\dot{\mathbf{v}}_{n+1} \\ \dot{\mathbf{u}}_{n+\xi_f} = \dot{\mathbf{u}}_n + \xi_f \Delta\dot{\mathbf{u}}_{n+1} \\ \mathbf{u}_{n+\xi_f} = \mathbf{u}_n + \xi_f \Delta\mathbf{u}_{n+1} \end{cases} \tag{23}$$

Now, combining these expressions and the following Newmark formulae [145]:

$$\begin{cases} \mathbf{u}_{n+1} = \mathbf{u}_n + h\dot{\mathbf{u}}_n + \left(\frac{1}{2} - \beta\right) h^2 \dot{\mathbf{v}}_n + \beta h^2 \dot{\mathbf{v}}_{n+1} \\ \dot{\mathbf{u}}_{n+1} = \dot{\mathbf{u}}_n + (1-\gamma) h\dot{\mathbf{v}}_n + \gamma h \dot{\mathbf{v}}_{n+1} \end{cases} \tag{24}$$

or similarly

$$\begin{cases} \Delta\dot{\mathbf{v}}_{n+1} = \frac{1}{\gamma h}\Delta\dot{\mathbf{u}}_{n+1} - \frac{1}{\gamma}\dot{\mathbf{v}}_n \\ \Delta\mathbf{u}_{n+1} = \frac{\beta h}{\gamma}\Delta\dot{\mathbf{u}}_{n+1} + h\dot{\mathbf{u}}_n + \frac{\gamma - 2\beta}{2\gamma} h^2 \dot{\mathbf{v}}_n \end{cases} \tag{25}$$

we obtain a new format for the generalized-α schemes with Lagrange multipliers:

$$\mathbf{K}^* \Delta\dot{\mathbf{u}}_{n+1} = \mathbf{g}_{n+1} + \mathbf{L}^t \mathbf{\Lambda}_{n+\xi_f} \tag{26}$$

with the following dynamics matrix operator:

$$\mathbf{K}^* = \xi_g \frac{1}{\gamma h}\mathbf{M} + \xi_f \frac{\beta h}{\gamma}\mathbf{K} \tag{27}$$

and the right-hand side vector $\mathbf{g}_{n+1}$ expressed as

$$\mathbf{g}_{n+1} = \mathbf{f}_{n+\xi_f} - \mathbf{K}\mathbf{u}_n - \xi_f h\mathbf{K}\dot{\mathbf{u}}_n - \left(1 - \frac{\xi_g}{\gamma}\right)\mathbf{M}\dot{\mathbf{v}}_n - \xi_f \left(\frac{\gamma - 2\beta}{2\gamma}\right) h^2 \mathbf{K}\dot{\mathbf{v}}_n \tag{28}$$

Here, the fundamental roles of ξ_g and ξ_f are clear: they consist of a separate ponderation on the mass matrix $\mathbf{M}$ and the stiffness matrix $\mathbf{K}$ (Equation (27)). In practice, Equations (25) and (26) are used for the numerical implementation of a given α-time integrator. It can be noticed that Equations (26)–(28) correspond to the Newmark time integrators with the following relationships: $\xi_g = \xi = \gamma$ and $\xi_f = \xi = \gamma$. Finally, it is interesting to adopt a compact form for the α-time integrators (with Lagrange multipliers) as a combination of (25) and (26):

$$\mathbb{K}^* \Delta\mathbb{U}_{n+1} = \mathbb{G}_{n+1} + \mathbb{L}^t \mathbf{\Lambda}_{n+\xi_f} \tag{29}$$

with the right-hand side vector given by

$$\mathbb{G}_{n+1} = \mathbb{F}_{n+\xi_f} - \mathbb{N}\mathbb{U}_n \tag{30}$$

The previous matrices and vectors involved in the compact form for the complete solving over time step h for all α-time integrators are given in the following:

$$\mathbb{K}^* = \begin{bmatrix} \mathbf{K}^* & \mathbf{0} & \mathbf{0} \\ -\frac{\beta h}{\gamma}\mathbf{I} & \mathbf{I} & \mathbf{0} \\ -\frac{1}{\gamma h}\mathbf{I} & \mathbf{0} & \mathbf{I} \end{bmatrix}, \ \mathbb{L}^t = \begin{bmatrix} \mathbf{L}^t \\ \mathbf{0} \\ \mathbf{0} \end{bmatrix} \tag{31}$$

$$\mathbb{U}_n = \begin{bmatrix} \dot{\mathbf{u}}_n \\ \mathbf{u}_n \\ \dot{\mathbf{v}}_n \end{bmatrix}, \ \Delta\mathbb{U}_{n+1} = \begin{bmatrix} \Delta\dot{\mathbf{u}}_{n+1} \\ \Delta\mathbf{u}_{n+1} \\ \Delta\dot{\mathbf{v}}_{n+1} \end{bmatrix} \tag{32}$$

$$\mathbb{F}_{n+\xi_f} = \begin{bmatrix} \mathbf{f}_{n+\xi_f} \\ \mathbf{0} \\ \mathbf{0} \end{bmatrix}, \mathbb{N} = \begin{bmatrix} \xi_f h\mathbf{K} & \mathbf{K} & \xi_f \left(\frac{\gamma - 2\beta}{2\gamma}\right) h^2\mathbf{K} + \left(1 - \frac{\xi_g}{\gamma}\right)\mathbf{M} \\ h\mathbf{I} & \mathbf{0} & \left(\frac{\gamma - 2\beta}{2\gamma}\right) h^2\mathbf{I} \\ \mathbf{0} & \mathbf{0} & -\frac{1}{\gamma}\mathbf{I} \end{bmatrix} \tag{33}$$

We recall that Newmark, Krenk, Simo, or Verlet time integrators for instance are particular cases of the compact form in Equation (29) with Lagrange multipliers (e.g., [145, 150]).

2.2. Stability analysis of ODE and DAE

As briefly described in the introduction, analysis of time integrators is necessary in order to understand the advantages and drawbacks of the various schemes dedicated to structural dynamics. Of particular importance are stability, accuracy, numerical dissipation, and overshoot. Typically, stability can be evaluated by an appropriate norm on the solution vector (displacement, velocity, and possibly acceleration), generally based on eigenvector orthogonality property (series of uncoupled SDOF systems) [25, 92, 102]. Classically, stability analysis is performed from the amplification matrix $\mathbf{A}$ defined as

$$\mathbf{X}_{n+1} = \mathbf{A}\mathbf{X}_n \tag{34}$$

where $\mathbf{X} \equiv (\mathbf{u}, \mathbf{v})$ is the considered state vector. For LMS methods, stability is governed by the so-called Dahlquist barrier where it is proven that there exists no unconditionally stable LMS methods with accuracy greater than order 2 [4] (e.g., Time Discontinuous Galerkin Integrators (TDG) integrators are not LMS integrators and are not concerned by this limit). Furthermore, most time integrators

for structural dynamics are A-stable, that is, unconditionally stable in the linear regime. However, it may not be sufficient to ensure a robust temporal integration. For instance, HHT-α can exhibit a low effectiveness of the numerical dissipation with possible overshoot [51]. In the same way, Hulbert and Hughes proved that the HHT-α time integrator suffers from the velocity overshoot and that the acceleration is only first-order accurate [25]. A better stability condition consists in L-stability. Indeed, it has been shown that this stability property does not exhibit overshoot [52]. L-stability combined with the optimized dissipation characteristics of higher modes represents the attractive properties in the linear regime of the CH-α method [45]. These properties can be user controlled by means of the spectral radius at infinity (ρ_∞) ($\rho_\infty = 0$ corresponds to the case of asymptotic annihilation of the high-frequency response, while $\rho_\infty = 1$ corresponds to the case of no numerical dissipation) (Table I). In fact, L-stability is related to high-frequency numerical dissipation and has been shown to be critical for solving problems of constrained nonlinear dynamics. More recently, the concept of Lyapunov exponents was also used to quantify the stability in structural dynamics [75]. Finally, the (energy) stability analysis suggested, among others, by Belytschko, Shoeberle, and Hughes is of great interest as it can be applied in nonlinear structural dynamics [6, 9]. It has to be noticed that the energy method does not require any state vector at a given time, which is of great interest for asynchronous time integrators. Indeed, the energy method proposed by Hughes has been widely used for obtaining the stability conditions for coupling schemes, mixing implicit and explicit schemes [24]. This is why, this nice property was used initially for the stability analysis of GC HATI [66, 74, 79, 88]. Furthermore, stability analysis of the PH method has also been proven this way [108]. It consists in proving that the interface pseudo-energy is equal or less than zero. Here, the interface pseudo-energy is employed as the starting point of the new coupling methods by seeking to ensure the zero-interface pseudo-energy. Thus, the following coupling schemes are built from the discrete balance equation given in the energy method in terms of pseudo-energy. For a given subdomain (by omitting the scripts for belonging subdomains), the pseudo-energy balance equation for the Newmark time integrator is given by [24]

$$\begin{aligned}\left[\frac{1}{2}\dot{\mathbf{v}}^t\mathbf{A}\dot{\mathbf{v}}+\frac{1}{2}\dot{\mathbf{u}}^t\mathbf{K}\dot{\mathbf{u}}\right]_n^{n+1} &= \frac{1}{h}\Delta\dot{\mathbf{u}}^t\left\{(\mathbf{f}_{n+1}-\mathbf{f}_n)\right\}\ldots \\ &\quad -\left(\gamma-\frac{1}{2}\right)\left\{\Delta\dot{\mathbf{v}}^t\mathbf{A}\Delta\dot{\mathbf{v}}\right\}\end{aligned} \tag{35}$$

where $\mathbf{A}$ is defined as

$$\mathbf{A}=\mathbf{M}+\left(\beta-\frac{\gamma}{2}\right)h^2\mathbf{K} \tag{36}$$

The previous balance equation can also be denoted as

$$\Delta E_{kin}+\Delta E_{int}=\Delta E_{ext}+\Delta E_{diss} \tag{37}$$

where ΔE_{kin}, ΔE_{int}, ΔE_{ext}, and ΔE_{diss} are the increments over the time step of kinetic, internal, external, and numerical dissipated pseudo-energies [24]. Based on an eigenvalue analysis of the matrix $\mathbf{A}$, we obtain very easily the stability property of the Newmark time integrator [88]. It can be noticed that the pseudo-energy method is dedicated to stability analysis of time integrators by studying the eigenvalues of operator $\mathbf{A}$ (Equation (36)). When Lagrange multipliers occur (DAE), the following interface pseudo-energy is added on the right-hand side of Equation (37) in the same way as the external pseudo-energy [90, 140, 151]:

$$\Delta E_{interface}=\frac{1}{h}\Delta\dot{\mathbf{u}}^t\left\{\mathbf{L}^t\left(\mathbf{\Lambda}_{n+1}-\mathbf{\Lambda}_n\right)\right\} \tag{38}$$

As already mentioned by Hughes [24] and all the papers based on the GC approach [88], the pseudo-energy method has to be distinguished from the discretized energy balance equation (Equations (72) and (74)). Indeed, here, the pseudo-energy is dedicated to stability analysis. Furthermore, the numerical energy balance equation is dedicated to the energy-preserving analysis of a given time integrator. A second comment concerns Equations (37) and (38): their combination consists in a

generalization of the pseudo-energy method (mainly dedicated to ODE, without Lagrange multipliers) to DAE (with Lagrange multipliers). This property is also confirmed by stability analysis based on amplification matrix applied to DAE with Lagrange multipliers (see Section 3.3 for details). In the next part, a new class of HATI will be introduced, from fundamental Equations (19) and (38).

3. HETEROGENEOUS ASYNCHRONOUS TIME INTEGRATORS

3.1. A state of the art of HATI

In the aim to surpass the classical approach (a unique time integrator and a unique timescale for the whole structure) for structural dynamics, many attempts in the past have consisted of developing HATI. Generally, it consists of cutting the considered structure into different subdomains individually handled by an appropriate time integrator with a chosen time step. Since the pioneer works of Belytschko and co-authors, much work has been performed in order to circumvent the barriers associated with a unique time integrator with a global time discretization. To relax the time step constraint imposed by stability requirements, mixed (heterogeneous) methods or multi-time (asynchronous) methods with different time steps for each domain were proposed. Belytschko and Mullen [7, 8, 12, 26] were the first to use a mixed explicit/implicit method with a nodal partition, while Hughes and Liu [11, 14] introduced a mixed method using an element partition. Belytschko and co-authors introduced subcycling for first-order problems and later extended it to non-integer time step ratios [15, 21]. Belytschko and others developed subcycling with non-integer ratios for second-order structural problems [14, 15, 18]. Although popular, the stability of second-order subcycling methods has been elusive. Smolinski and Sleith proposed an explicit subcycling algorithm for second-order problems that was proven stable but is less accurate than other algorithms [38, 39, 55, 78]. The multi-timescale features of theses approaches often suffer from stability difficulties as soon as subcycling is activated, explained by the need of interpolated values at the interface between the subdomains from the fine timescale to the coarse timescale. This drawback of subcycling algorithms has been discussed by several authors such as Belytschko and Lu [42, 43], Klisinski and Mostrom [64], and Daniel [59, 61–63, 99, 100] who showed that multi-time-step algorithms coupling explicit integration schemes lead to narrow bands of possible unstable time steps, smaller than the expected stability limit (statistical stability [49]). Wu and Smolinski [67, 78] proposed a new explicit multi-time strategy (mE/E) for solving structural dynamics problems derived from the modified trapezoidal rule method. Stability has been analyzed with the so-called energy method originally introduced by Hughes for hybrid explicit/implicit coupling algorithm [24]; stability has been well achieved, but investigated dynamics problems highlight accuracy difficulties for a rather small time step ratio of less than 10. Recently, an optimization of the multi-timescale approach involving only explicit time integration schemes has been achieved, by associating a local time step with each finite element composing the whole domain [134]. Local time integration is also available for variational integrators (e.g., [153]). All these former coupling algorithms can be classified in a primal approach in the sense that subdomains are linked on the interface nodes (or elements) with a displacement continuity property.

Theoretically, in order to build the space–time discretized weak formulation, it is possible to choose between displacement, velocity, and acceleration continuity at the interface. Indeed, for the discretized formulation in time, they are only equivalent when the time step tends to zero. This is why dual approaches are of great interest in their ability to prescribe the continuity of a given kinematic quantity of interest by the use of Lagrange multipliers (e.g., Equation (19)). The GC method, proposed by Gravouil and Combescure [88, 90], has been then built in this framework with a velocity continuity at the interface at the finest timescale in order to build a general class of HATI. The authors showed that any Newmark time integrator can be coupled (explicit or implicit) with their own timescale, providing a general demonstration of stability using the energy method (Section 2.2) [24, 88, 90]. Nonetheless, energy dissipation can occur as soon as different timescales are considered, leading to a global first-order accuracy when second-order time integrators are used.

Many engineering applications of this method are available for transient nonlinear dynamics, FSI, non-matching interfaces, co-computations, simulation of automobile crashes, hybrid experimen-

tal/numerical real-time testing, earthquake loading, impact on concrete structures, microsystems, coupled electro-mechanical problems, and fracture in polysilicon micro electro-mechanical systems, with two or more subdomains with their own integrator and timescale [60, 66, 74, 79, 88, 90, 93, 94, 96, 97, 103–107, 116, 131, 132, 140–142, 145, 148–152, 154, 157–161, 164–166] (see for instance [145] for an example with nine subdomains, nine different time integrators, and a maximum ratio of time steps close to 1000).

Recently, further efforts have been carried out to build coupling methods able to handle the generalized-α schemes proposed by Chung and Hulbert [45], well known for being able to control numerical damping and to filter out spurious high-frequency components of the response. The low frequencies are unaffected, and the time integrator remains second-order accurate. Bursi *et al.* [143] underline that the GC method based on the velocity continuity at the end time of the fine time steps is incompatible with the generalized-α scheme whose terms involved into the equation of motion are weighted by different parameters. Therefore, in order to adapt the generalized-α scheme to the end time collocation format of the GC coupling method, a new form of the generalized-α scheme proposed by Arnold and Bruls [122] in the multibody dynamics context is adopted, enforcing the equilibrium at the end of the time step instead of an averaged form as in the original time integrator. The derived interfield parallel solution method, called the PM-α method, is an extension to the α-schemes of the PM method [143].

Built upon the GC formulation, two other multi-time coupling schemes have been proposed. The first one is the PH method developed by Prakash and Hjelmstad [108, 167], assuming a velocity continuity on the interface at the macro timescale (large time step) unlike the GC method based on the micro timescale (fine time step). It enables the dissipative drawback of the GC method to be tackled while optimizing the computation time related to the solving of the interface problem. The authors proved by using the energy method that the pseudo-energy at the interface remains equal to zero (Equation (38)). They concluded that the PH method is energy conserving when coupling non-dissipative Newmark schemes such as the implicit constant average acceleration (CAA) scheme and the explicit central difference (CD) scheme. Recently, the Mahjoubi Gravouil Combescure (MGC) method (based on a similar macro timescale velocity continuity assumption) has been built in order to be able to couple the Newmark schemes, HHT-α scheme [10], Simo scheme [37], and Krenk scheme (balance dissipation scheme, [111, 118, 120, 125, 130]) in linear dynamics [141, 145]. In other words, the MGC method can be seen as an extension of the PH method to the HHT-α scheme. Nonetheless, the MGC coupling method uses a modified equation of motion for the HHT-α scheme: solving the equation of motion related to a given time step requires quantities one time step before, losing the single-solve single-step format of the original HHT-α scheme. More generally, recent works propose asynchronous variational time integrators for structural dynamics [101, 127, 129]. Furthermore, there are some attempts for heterogeneous asynchronous variational time integrators for nonlinear structural dynamics; however, they reveal to be conditionally stable [144]. More generally, truly (homogeneous) asynchronous variational integrators are now available in that different time step can be chosen at each element, generalizing the subcycling approach, with possible contact nonlinearities [126, 153]. In the same way, FSI problems often require heterogeneous asynchronous time integrators. For such applications, we can distinguish partitioned and monolithic approaches, with specific integrators and timescales for the solid and fluid parts. A very good state of the art for both partitioned and monolithic approaches can be found for instance in references [17, 30, 33, 46, 68, 73, 80, 81, 95, 115, 123, 124]. Drawbacks and advantages of partitioned and monolithic approaches are still studied in detail, in terms of stability, accuracy, and computational cost [95, 155]. It can be noticed that a generalization of the GC method has been applied recently with success to FSI [161]. Finally, one can also mention overlapping methods as an alternative for the development of HATI for specific applications such as multiscale physics, continuum/molecular dynamics coupling [23, 121, 128, 136].

In this paper, two new BGC (Brun Gravouil Combescure) coupling methods, denoted in the following BGC-macro and BGC-micro methods, will be derived by seeking to cancel the interface pseudo-energy. The BGC-macro method is a macro-time-based method, such as the PH and MGC methods [108, 140–142, 145]. It assumes a linear variation of the Lagrange multipliers over the macro time step so as to lead to a kinematic condition at the interface, which,

used together with the Lagrange multiplier variation assumption, guarantees the zero value of the interface pseudo-energy. It will be shown that the new method exactly matches the PH method when considering Newmark schemes but can also be easily extended to the α-schemes (HHT-α [10], WBZ-α [16], and CH-α [45]) unlike the PH method. The BGC-micro method is micro time based in the sense that the interface problem is handled at the micro timescale. It generalizes the GC progenitor method of this family of hybrid (different types of integrator) multi-time-step coupling schemes: the new micro-based coupling method exactly matches the GC method for Newmark schemes but can also be employed for the α-schemes. In addition, it is important to note that the α-schemes are employed without modifying the original formulation, unlike what has been carried out previously for the PM-α and MGC algorithms [140–142, 145].

3.2. On dual HATI

3.2.1. A general class of dual HATI based on energetic considerations. We propose here a general framework of dual HATI based on weak velocity continuity in time and energy considerations from fundamental expressions (19) and (38). Assuming two subdomains Ω_A and Ω_B ($\Omega_A \cap \Omega_B = \emptyset$) with their own time integrator and timescale, which are respectively coarse and fine, we can introduce the following action integral based on the three-field stationary principle (16) over the macro time step $h_A = [t_0; t_m]$:

$$\begin{aligned}
&\delta\tilde{\mathcal{A}} = 0 \\
&\Leftrightarrow -\int_{t_0}^{t_m} \delta\mathbf{u}^{A^t}(t)\left(\mathbf{M}_A\dot{\mathbf{v}}^A(t) + \mathbf{K}_A\mathbf{u}^A(t) - \mathbf{f}_A(t) - \mathbf{L}_A^t\Lambda(t)\right)\mathrm{d}t \\
&\quad -\int_{t_0}^{t_m} \delta\mathbf{u}^{B^t}(t)\left(\mathbf{M}_B\dot{\mathbf{v}}^B(t) + \mathbf{K}_B\mathbf{u}^B(t) - \mathbf{f}_B(t) - \mathbf{L}_B^t\Lambda(t)\right)\mathrm{d}t \\
&\quad +\int_{t_0}^{t_m} \delta\lambda^t(t)\left(\mathbf{L}_A\dot{\mathbf{u}}^A(t) + \mathbf{L}_B\dot{\mathbf{u}}^B(t)\right)\mathrm{d}t = 0
\end{aligned} \tag{39}$$

In order to consider a large class of time integrators, we follow the approach proposed by Crisfield, Tamma, and co-authors (Section 2.1). In this way, we can choose for each subdomains Ω_A and Ω_B a time integrator based on α-schemes (e.g., HHT-α, WBZ-α, and CH-α). It involves the following set of seven equations, with eight numerical parameters $\gamma_A, \beta_A, \xi_{A,f}, \xi_{A,g}$ and $\gamma_B, \beta_B, \xi_{B,f}, \xi_{B,g}$, with the two coarse and fine time steps h_A and h_B, respectively (see Section 2.1 and Equations (22) and (25)–(28) for the definition of these time integrator parameters):

$$\begin{cases}
\mathbf{K}_A^*\Delta\dot{\mathbf{u}}_m^A = \mathbf{g}_m^A + \mathbf{L}_A^t\boldsymbol{\Lambda}_{n+\xi_A,f} \\
\Delta\mathbf{u}_m^A = \frac{\beta_A h_A}{\gamma_A}\Delta\dot{\mathbf{u}}_m^A + h_A\dot{\mathbf{u}}_0^A + \frac{\gamma_A - 2\beta_A}{2\gamma_A}h_A^2\dot{\mathbf{v}}_0^A \\
\Delta\dot{\mathbf{v}}_m^A = \frac{1}{\gamma_A h_A}\Delta\dot{\mathbf{u}}_m^A - \frac{1}{\gamma_A}\dot{\mathbf{v}}_0^A
\end{cases} \tag{40}$$

$$\begin{cases}
\mathbf{K}_B^*\Delta\dot{\mathbf{u}}_j^B = \mathbf{g}_j^B + \mathbf{L}_B^t\boldsymbol{\Lambda}_{j-1+\xi_B,f} \\
\Delta\mathbf{u}_j^B = \frac{\beta_B h_B}{\gamma_B}\Delta\dot{\mathbf{u}}_j^B + h_B\dot{\mathbf{u}}_{j-1}^B + \frac{\gamma_B - 2\beta_B}{2\gamma_B}h_B^2\dot{\mathbf{v}}_{j-1}^B \\
\Delta\dot{\mathbf{v}}_j^B = \frac{1}{\gamma_B h_B}\Delta\dot{\mathbf{u}}_j^B - \frac{1}{\gamma_B}\dot{\mathbf{v}}_{j-1}^B \\
\forall j \in \{1, m\}
\end{cases} \tag{41}$$

$$\int_{t_0}^{t_m} \mathbf{L}_A\dot{\mathbf{u}}^A(t) + \mathbf{L}_B\dot{\mathbf{u}}^B(t)\,\mathrm{d}t = 0 \tag{42}$$

where Equations (40) and (41) correspond to weak equilibrium equation in time on the coarse and fine timescales for subdomains Ω_A and Ω_B, respectively. Here, for simplicity, we assume that

$h_A = mh_B$ (more complex cases have to be investigated [129]). Then, the preceding equations can also be given in a compact form as (Equation (29))

$$\begin{cases} \mathbb{K}_A^* \Delta \mathbb{U}_m^A = \mathbb{F}_{\gamma_A}^A - \mathbb{N}_A \mathbb{U}_0^A + \mathbb{L}_A^t \mathbf{\Lambda}_{\xi_A, f} \\ \mathbb{K}_B^* \Delta \mathbb{U}_j^B = \mathbb{F}_{j-1+\gamma_B}^B - \mathbb{N}_B \mathbb{U}_{j-1}^B + \mathbb{L}_B^t \mathbf{\Lambda}_{j-1+\xi_B, f} \ \forall j \in \{1, m\} \\ \int_{t_0}^{t_m} \mathbf{L}_A \dot{\mathbf{u}}^A(t) + \mathbf{L}_B \dot{\mathbf{u}}^B(t) \, \mathrm{d}t = 0 \end{cases} \tag{43}$$

Finally, the last step consists of building the discretized form of the velocity continuity at the interface between Ω_A and Ω_B (see the last equation in (43)). For that purpose, the energy balance based on the energy method (Section 2.2) is applied to the whole structure based on subdomains Ω_A and Ω_B plus the interface over the macro time step $h_A = [t_0; t_m]$:

$$\begin{gathered} \Delta E_{kin,m}^A + \Delta E_{int,m}^A + \sum_{j=1}^{m} \left\{ \Delta E_{kin,j}^B + \Delta E_{int,j}^B \right\} = \cdots \\ \left(\Delta E_{ext,m}^A + \sum_{j=1}^{m} \Delta E_{ext,j}^B \right) + \left(\Delta E_{diss,m}^A + \sum_{j=1}^{m} \Delta E_{diss,j}^B \right) + \Delta E_{interface} \end{gathered} \tag{44}$$

The interface pseudo-energy can be written as (Equation (38))

$$\Delta E_i = \frac{1}{h_A} \Delta \dot{\mathbf{u}}_m^{A\,t} \left\{ \mathbf{L}_A^t \left(\mathbf{\Lambda}_m - \mathbf{\Lambda}_0 \right) \right\} + \sum_{j=1}^{m} \left\{ \frac{1}{h_B} \Delta \dot{\mathbf{u}}_j^{B\,t} \left\{ \mathbf{L}_B^t \left(\mathbf{\Lambda}_j - \mathbf{\Lambda}_{j-1} \right) \right\} \right\} \tag{45}$$

Assuming that the considered time integrators are α-schemes, then a linear interpolation from the coarse timescale to the fine one (on the interface between subdomains Ω_A and Ω_B) can be used (see the last equation in (20)):

$$\mathbf{\Lambda}_j = \left(1 - \frac{j}{m} \right) \mathbf{\Lambda}_0 + \frac{j}{m} \mathbf{\Lambda}_m \tag{46}$$

Historically, this equation was seen as a supplementary condition added to the set of Equation (43) [88]. However, more generally, it can be seen as a fundamental property of α time integrators with Lagrange multipliers (Equation (20)). In other words, it is no more than a general property of α-schemes with Lagrange multipliers used as a natural approach for dual HATI. As a consequence, we can write

$$\mathbf{\Lambda}_j - \mathbf{\Lambda}_{j-1} = \frac{1}{m} \left(\mathbf{\Lambda}_m - \mathbf{\Lambda}_0 \right) \tag{47}$$

Then, the interface pseudo-energy can be simplified as

$$\Delta E_{interface} = \left[\frac{1}{h_A} \Delta \dot{\mathbf{u}}_m^{A\,t} \mathbf{L}_A^t + \sum_{j=1}^{m} \left\{ \frac{1}{m h_B} \Delta \dot{\mathbf{u}}_j^{B\,t} \mathbf{L}_B^t \right\} \right] \left(\mathbf{\Lambda}_m - \mathbf{\Lambda}_0 \right) \tag{48}$$

Finally, the zero-interface pseudo-energy requirement $\Delta E_{interface} = 0$ (for stability considerations) leads to the two possible kinematic equations:

$$\mathbf{L}_A \Delta \dot{\mathbf{u}}_m^A + \sum_{j=1}^{m} \mathbf{L}_B \Delta \dot{\mathbf{u}}_j^B = 0 \tag{49}$$

or

$$\frac{1}{m} \mathbf{L}_A \Delta \dot{\mathbf{u}}_m^A + \mathbf{L}_B \Delta \dot{\mathbf{u}}_j^B = 0 \tag{50}$$

The first kinematic Equation (49) is the basis of BGC-macro dual HATI [168] where velocity continuity is ensured at the macro timescale between Ω_A and Ω_B.

As already mentioned in this paper, the proposed pseudo-energy approach is a generalization of the ODE stability analysis (without Lagrange multipliers) to the DAE stability analysis (with Lagrange multipliers). This can be confirmed by an amplification matrix stability analysis (see Section 3.3 for details). As a consequence, if the interface pseudo-energy (48) is zero or negative, then the global stability of the HATI is ensured. In other words, each time integrator of each subdomain keeps its own stability property (independently on the interface). It is interesting also to notice that only properties (47) and (49) are required for building BGC-macro dual HATI. Indeed, PH methods (which are particular cases of BGC-macro dual HATI to Newmark) are built historically on unnecessary assumptions (linearity of displacement, velocity, and acceleration fields). Now, the same result can be obtained without these assumptions (see also [145, 151, 163, 164, 168]). Finally, the second kinematic Equation (50) is the basis of BGC-micro dual HATI [168] where velocity continuity is ensured at the micro timescale between Ω_A and Ω_B. The GC method can be seen as a particular BGC-micro dual HATI for Newmark, where a stability analysis was obtained for the first time by the pseudo-energy method [88, 90].

In the next two subsections, we will define the specificities of BGC-macro and BGC-micro dual HATI in terms of algorithmic implementation [168].

3.2.2. BGC-macro dual HATI. It is now time to write a general framework of dual HATI based on velocity continuity at the macro timescale and energy considerations in a compact form (Equations (43) and (49)):

$$\begin{cases} \mathbb{K}_A^* \Delta \mathbb{U}_m^A = \mathbb{F}_{\gamma_A}^A - \mathbb{N}_A \mathbb{U}_0^A + \mathbb{L}_A^t \mathbf{\Lambda}_{\xi_A,f} \\ \mathbb{K}_B^* \Delta \mathbb{U}_j^B = \mathbb{F}_{j-1+\gamma_B}^B - \mathbb{N}_B \mathbb{U}_{j-1}^B + \mathbb{L}_B^t \mathbf{\Lambda}_{j-1+\xi_B,f} \ \forall j \in \{1,m\} \\ \mathbf{L}_A \Delta \dot{\mathbf{u}}_m^A + \sum_{j=1}^m \mathbf{L}_B \Delta \dot{\mathbf{u}}_j^B = 0 \end{cases} \tag{51}$$

It is clear that this set of Equation (51) is fully coupled on the macro timescale. This is why it is required to propose a global formulation in time. For that purpose, we introduce the following notations:

$$\begin{cases} \mathbf{E}_{A,m}^t = \left(1-\xi_{A,f}\right)\mathbf{L}_A^t \\ \mathbf{C}_{A,m}^t = \xi_{A,f}\mathbf{L}_A^t \\ \mathbf{E}_{B,j}^t = \left[\left(1-\xi_{B,f}\right)\left(1-\frac{j-1}{m}\right)+\xi_{B,f}\left(1-\frac{j}{m}\right)\right]\mathbf{L}_B^t \\ \mathbf{C}_{B,j}^t = \left[\left(1-\xi_{B,f}\right)\left(\frac{j-1}{m}\right)+\xi_{B,f}\left(\frac{j}{m}\right)\right]\mathbf{L}_B^t \quad \forall j \in [1,m] \end{cases} \tag{52}$$

and

$$\mathbb{L}_A = \left[\mathbf{L}_A \ \mathbf{0} \ \mathbf{0}\right] \ , \ \mathbb{L}_B = \left[\mathbf{L}_B \ \mathbf{0} \ \mathbf{0}\right] \tag{53}$$

The matrices $\mathbb{C}_{A,m}$ and $\mathbb{E}_{A,m}$ related to the subdomain Ω_A are given by

$$\mathbb{C}_{A,m} = \left[\mathbf{C}_{A,m} \ \mathbf{0} \ \mathbf{0}\right] \ , \ \mathbb{E}_{A,m} = \left[\mathbf{E}_{A,m} \ \mathbf{0} \ \mathbf{0}\right] \tag{54}$$

whereas the matrices $\mathbb{C}_{B,j}$ and $\mathbb{E}_{B,j}$ related to the subdomain Ω_B are

$$\mathbb{C}_{B,j} = \left[\mathbf{C}_{B,j} \ \mathbf{0} \ \mathbf{0}\right] \ , \ \mathbb{E}_{B,j} = \left[\mathbf{E}_{B,j} \ \mathbf{0} \ \mathbf{0}\right] \quad \forall j \in [1,m] \tag{55}$$

Then, the global system of equilibrium equations is obtained by gathering the compact forms of the three-stage time-stepping schemes for both subdomains. It writes

$$\left[\begin{array}{ccccc|c|c} \mathbb{K}_B^* & & & & & & \mathbb{C}_{B,1}^t \\ \mathbb{N}_B & \mathbb{K}_B^* & & & & & -\mathbb{C}_{B,2}^t \\ \mathbb{N}_B & \mathbb{N}_B & \mathbb{K}_B^* & & & & -\mathbb{C}_{B,3}^t \\ & \ddots & \ddots & \ddots & & & \vdots \\ \mathbb{N}_B & \mathbb{N}_B & \mathbb{N}_B & \mathbb{N}_B & \mathbb{K}_B^* & & -\mathbb{C}_{B,m}^t \\ \hline & & & & & \mathbb{K}_A^* & -\mathbb{C}_{A,m}^t \\ \hline -\mathbb{L}_B & -\mathbb{L}_B & -\mathbb{L}_B & \cdots & -\mathbb{L}_B & -\mathbb{L}_A & \mathbf{0} \end{array}\right] \left[\begin{array}{c} \Delta\mathbb{U}_1^B \\ \Delta\mathbb{U}_2^B \\ \Delta\mathbb{U}_3^B \\ \vdots \\ \Delta\mathbb{U}_m^B \\ \hline \Delta\mathbb{U}_m^A \\ \hline \boldsymbol{\Lambda}_m \end{array}\right] = \left[\begin{array}{c} \mathbb{F}_{\xi_{B,f}}^B - \mathbb{N}_B\mathbb{U}_0^B + \mathbb{E}_{B,1}^t\boldsymbol{\Lambda}_0 \\ \mathbb{F}_{1+\xi_{B,f}}^B - \mathbb{N}_B\mathbb{U}_0^B + \mathbb{E}_{B,2}^t\boldsymbol{\Lambda}_0 \\ \mathbb{F}_{2+\xi_{B,f}}^B - \mathbb{N}_B\mathbb{U}_0^B + \mathbb{E}_{B,3}^t\boldsymbol{\Lambda}_0 \\ \vdots \\ \mathbb{F}_{m-1+\xi_{B,f}}^B - \mathbb{N}_B\mathbb{U}_0^B + \mathbb{E}_{B,m}^t\boldsymbol{\Lambda}_0 \\ \hline \mathbb{F}_{\xi_{A,f}}^A - \mathbb{N}_A\mathbb{U}_0^A + \mathbb{E}_{A,m}^t\boldsymbol{\Lambda}_0 \\ \hline \mathbf{0} \end{array}\right] \tag{56}$$

Then, the BGC-macro HATI is composed of the following blocks:

$$\left[\begin{array}{cc} K & -L^t \\ B & \mathbf{0} \end{array}\right] \left[\begin{array}{c} \Delta U \\ \Lambda \end{array}\right] = \left[\begin{array}{c} F \\ \mathbf{0} \end{array}\right] \tag{57}$$

It can be solved by a bordering approach, by decomposing the quantities into free and linked quantities as $\Delta U = \Delta U_{free} + \Delta U_{link}$. The bordering approach can be seen as a predictor–corrector method. By splitting the system into free and link problems, the global system becomes

$$\begin{cases} K\Delta U_{free} = F \\ H\Lambda = -B\Delta U_{free} \quad \text{with } H = \left[BK^{-1}L^t\right] \\ K\Delta U_{link} = L^t\Lambda \end{cases} \tag{58}$$

More details about the solving of the global system and the building of the interface Steklov–Poincaré operator H can be found in [108, 140]. The BGC-macro integrator can be seen as a generalization of PH and MGC HATI to general α-integrators. Some numerical examples of this dual HATI will be presented in Section 4.

3.2.3. BGC-micro dual HATI. In this subsection, we propose an alternative class of dual HATI methods based on velocity continuity at the micro timescale between the subdomains Ω_A and Ω_B. From Equations (43) and (50), one obtains

$$\begin{cases} \mathbb{K}_A^*\Delta\mathbb{U}_m^A = \mathbb{F}_{\gamma_A}^A - \mathbb{N}_A\mathbb{U}_0^A + \mathbb{L}_A^t\boldsymbol{\Lambda}_{\xi_A,f} \\ \mathbb{K}_B^*\Delta\mathbb{U}_j^B = \mathbb{F}_{j-1+\gamma_B}^B - \mathbb{N}_B\mathbb{U}_{j-1}^B + \mathbb{L}_B^t\boldsymbol{\Lambda}_{j-1+\xi_B,f} \ \forall j \in \{1,m\} \\ \frac{1}{m}\mathbf{L}_A\Delta\dot{\mathbf{u}}_m^A + \mathbf{L}_B\Delta\dot{\mathbf{u}}_j^B = 0 \end{cases} \tag{59}$$

The Lagrange multipliers are computed at times $t_0 + \xi_{A_f}$ and $t_{j-1} + \xi_{B_f}$ for subdomains Ω_A and Ω_B as

$$\begin{cases} \boldsymbol{\Lambda}_{\xi_{A,f}} = \boldsymbol{\Lambda}_0 + \xi_{A,f}\,(\boldsymbol{\Lambda}_m - \boldsymbol{\Lambda}_0) \\ \boldsymbol{\Lambda}_{j-1+\xi_{B,f}} = \boldsymbol{\Lambda}_{j-1} + \xi_{B,f}\Delta\boldsymbol{\Lambda}_j \end{cases} \tag{60}$$

In this case, the set of Equation (59) is not fully coupled at the macro timescale; then an explicit formulation can be built at the micro timescale. Indeed, by splitting the quantities into free and linked quantities on the micro time step, the kinematic equation can be rewritten as

$$\frac{1}{m}\mathbf{L}_A\Delta\dot{\mathbf{u}}_{link,m}^A + \mathbf{L}_B\Delta\dot{\mathbf{u}}_{link,j}^B = -\frac{1}{m}\mathbf{L}_A\Delta\dot{\mathbf{u}}_{free,m}^A - \mathbf{L}_B\Delta\dot{\mathbf{u}}_{free,j}^B \tag{61}$$

The link problem for both subdomains can be derived as follows:

$$\begin{cases} \mathbf{K}_A^* \Delta \dot{\mathbf{u}}_{link,m}^A = \mathbf{L}_A^t \mathbf{\Lambda}_{\xi_{A,f}} \\ \mathbf{K}_B^* \Delta \dot{\mathbf{u}}_{link,j}^B = \mathbf{L}_B^t \mathbf{\Lambda}_{j-1+\xi_{B,f}} \end{cases} \tag{62}$$

Using Equation (62) and substituting the relationships concerning the Lagrange multipliers (47) and (60) into the kinematic relation (61), we obtain the interface Equation (58) for BGC-micro HATI with α-schemes:

$$\mathbf{H} \Delta \mathbf{\Lambda}_j = -\mathbf{b}_j \tag{63}$$

where the interface operator at the micro timescale and the right-hand side vector are defined by

$$\begin{cases} \mathbf{H} = \left[\xi_{A,f} \mathbf{L}_A (\mathbf{K}_A^*)^{-1} \mathbf{L}_A^t + \xi_{B,f} \mathbf{L}_B (\mathbf{K}_B^*)^{-1} \mathbf{L}_B^t \right] \\ \mathbf{b}_j = \frac{1}{m} \mathbf{L}_A \Delta \dot{\mathbf{u}}_{free,m}^A + L_B \Delta \dot{\mathbf{u}}_{free,j}^B - \frac{1}{m} \mathbf{L}_A (\mathbf{K}_A^*)^{-1} \mathbf{L}_A^t \mathbf{\Lambda}_0 - \mathbf{L}_B (\mathbf{K}_B^*)^{-1} \mathbf{L}_B^t \mathbf{\Lambda}_{j-1} \end{cases} \tag{64}$$

The interface equation has to be solved at each micro time step for computing the Lagrange multipliers at the micro timescale. It has to be underlined that, for linking the Lagrange multipliers at the macro timescale $\mathbf{\Lambda}_{\xi_{A,f}}$ to the micro timescale $\mathbf{\Lambda}_{j-1+\xi_{B,f}}$, the assumption of a constant Lagrange multiplier increment $\Delta \mathbf{\Lambda}$ has been adopted. This assumption will not be verified exactly into the computations because the Lagrange multiplier increment $\Delta \mathbf{\Lambda}_j$ is computed at every micro time step. In other words, contrary to the BGC-macro dual HATI integrator, the numerical variation of the Lagrange multipliers at the micro timescale cannot be accurately controlled. So, this micro timescale method fails to ensure the zero-energy dissipation at the interface in the sense of the energy method (see for instance numerical applications in Figure 6). On the opposite, the BGC-macro method requires a single solve of the interface problem at the macro timescale for obtaining the final Lagrange multiplier $\mathbf{\Lambda}_m$. The Lagrange multiplier at the micro timescale $\mathbf{\Lambda}_{j-1+\xi_{B,f}}$ is then directly interpolated from the initial and final Lagrange multipliers $\mathbf{\Lambda}_0$ and $\mathbf{\Lambda}_m$. As a result, it allows an accurate control of the Lagrange multipliers over the macro time step, enabling us to maintain the interface pseudo-energy at the zero value. Despite the overhead coming from the building of a more complex interface operator H, the BGC-macro method is a conservative energy coupling algorithm in the sense of the energy method and provides a greater computational efficiency as well as some advanced parallel capabilities. Indeed, the free computations can be conducted in a complete concurrent way for both subdomains, independently from each other. The dissipated interface energy drawback has been recognized by the authors of the progenitor GC method as soon as different timescales are considered; even a general proof of stability was obtained based on the pseudo-energy method (Section 2.2) [88] or by numerical analysis (Figure 6):

$$\begin{array}{l} \Delta E_{i\,BGC\text{-}macro} = 0 \\ \Delta E_{i\,BGC\text{-}micro} \leqslant 0 \end{array} \tag{65}$$

In the next subsection, a confirmation of pseudo-energy stability analysis is performed by the amplification matrix for BGC-macro HATI. This new general result was obtained only recently by Brun *et al.* [168], and based on the previous stability analysis developed in [132] and [143] for the PM method (a particular case of BGC-micro HATI close to GC).

3.3. Stability analysis of the BGC-micro and macro dual HATI by the amplification matrix

In the previous section, it has been shown that BGC-macro HATI preserves exactly the interface pseudo-energy by construction. This ensures the global stability of the HATI. Furthermore, it has been shown theoretically and numerically that BGC-micro HATI ensures a zero-interface or negative-interface pseudo-energy by construction. This also ensures the global stability of the corresponding HATI, with possible numerical damping. Here, a confirmation of these stability properties is carried out by the amplification matrix (Equation (34)). Historically, the amplification matrix stability analysis for DAE such as GC or PM was performed for the first time by Bonelli and coauthors [132, 143]. In other words, they have proposed a proof of stability by the amplification

matrix for a large class of BGC-micro HATI. This result is a clear confirmation of the previous stability analysis based on the pseudo-energy.

In the following, we also propose to confirm the previous pseudo-energy stability analysis of BGC-macro HATI by the amplification matrix as already performed by Brun *et al.* [168]. Along the lines of [132] and [143], an alternative convergence analysis is investigated here by building an amplification matrix $\mathbf{A}$ linking a state vector at time $t_n + h_A = t_{n+1}$ to the previous state vector at time t_n. The convergence of the BGC-macro method is carried out for a SDOF system, split into two subdomains Ω_A and Ω_B. In the same way, the BGC-macro method is recast into the following recursive form (external forces are assumed null as they do not influence the stability properties):

$$\mathbf{X}_{n+1} = \mathbf{A}\mathbf{X}_n \tag{66}$$

where $\mathbf{X}$ is an appropriate state vector depending on the formulation of the time integration algorithm, $\mathbf{A}$ is the amplification matrix. The BGC-macro method adopts the following state vector at time t_n:

$$\mathbf{X}_n = \left[\mathbf{X}_n^A \;\; \mathbf{X}_n^B\right]^T = \left[\mathbf{u}_n^A \;\; \dot{\mathbf{u}}_n^A \;\; h_A\dot{\mathbf{v}}_n^A \;\; h_A\boldsymbol{\lambda}_n \;\; \mathbf{u}_n^B \;\; \dot{\mathbf{u}}_n^B \;\; h_A\dot{\mathbf{v}}_n^B\right]^T \tag{67}$$

where $\mathbf{X}_n^A$ and $\mathbf{X}_n^B$ are the state vectors related the subdomains Ω_A and Ω_B, respectively. $\mathbf{X}_n^A$ collects the kinematic quantities of subdomain Ω_A, including the Lagrange multiplier at the macro timescale, and $\mathbf{X}_n^B$ collects the kinematic quantities of subdomain Ω_B. It is important to remark that the state vector includes the Lagrange multiplier contrary to the PM method proposed by Bonelli *et al*. [132] and Bursi *et al*. [143], including instead the free velocity related to the subdomain Ω_A. In [168], it has been proven that Equation (66) can be developed as

$$\begin{bmatrix} \mathbf{X}_{n+1}^A \\ \mathbf{X}_{n+1}^B \end{bmatrix} = \begin{bmatrix} \mathbf{A}^{AA} & \mathbf{A}^{AB} \\ \mathbf{A}^{BA} & \mathbf{A}^{BB} \end{bmatrix} \begin{bmatrix} \mathbf{X}_n^A \\ \mathbf{X}_n^B \end{bmatrix} \tag{68}$$

where the matrices $\mathbf{A}^{AA}$, $\mathbf{A}^{AB}$, $\mathbf{A}^{BA}$, and $\mathbf{A}^{BB}$ depend on the time step ratio. The absolute stability of the BGC-macro method is investigated by computing the seven eigenvalues of the amplification matrix $\mathbf{A}$ in the case of the split oscillator. The eigenvectors are linearly independent for each repeated eigenvalue λ_i. Hence, the condition $|\lambda_i| \leqslant 1$, for $i = 1, \ldots, 7$, is sufficient to demonstrate the A-stability of the method. In Figure 1, the coupling between two CH-α schemes (spectral radius $\rho_\infty = 0.8$ and $\rho_\infty = 0.5$ for each scheme) is investigated as a function of the time step ratio m by plotting the absolute values of the eigenvalues as a function of the reduced angular frequency $\Omega_B = \omega_B h_B$. Among the seven eigenvalues, only one pair is complex conjugate, giving the principal eigenvalues, whereas the five remaining are the spurious ones. In all investigated cases (any ρ_∞ and b_1), the BGC-macro method is found to be unconditionally stable when coupling unconditionally stable time integrators. In the following, the local truncation error τ_n is defined as

$$\tau_n = \mathbf{A}\mathbf{X}(t_n) - \mathbf{X}(t_{n+1}) \tag{69}$$

where $\mathbf{X}(t_n)$ and $\mathbf{X}(t_{n+1})$ correspond to the exact solutions of the state vector at times t_n and t_{n+1}. From numerical calculations, the order of the truncation error can be assessed by computing the slope of $\ln(\tau_n)$ as a function of the macro time step h_A. Indeed, the power k of the leading term of the local truncation error $\tau_n = \alpha h_A^k + O(h_A^{k+1})$ (α being constant) can be computed as $k = \frac{\ln(\tau_n(h_{2,A})) - \ln(\tau_n(h_{1,A}))}{\ln(h_{2,A}) - \ln(h_{1,A})}$, where $\tau_n(h_{2,A})$ and $\tau_n(h_{1,A})$ are the numerical results of the local truncation error for two different small values of the macro time step h_A, with $h_{1,A} < h_{2,A}$. One obtains

$$\tau_n = O(h_A^3) \tag{70}$$

for any values of the time step ratio m. It is worth noting that the same result has been obtained in [132] (Newmark schemes) and [143] (α-schemes) for their proposed PM method, but only in the case of the same time step in both subdomains. Indeed, as soon as different time steps are adopted, the PM method only exhibits $\tau_n = O(h_A^2)$. For illustration, the local truncation error is plotted in Figure 2 for a time step ratio $m = 2$. It can be seen that the power k of the leading term of the local

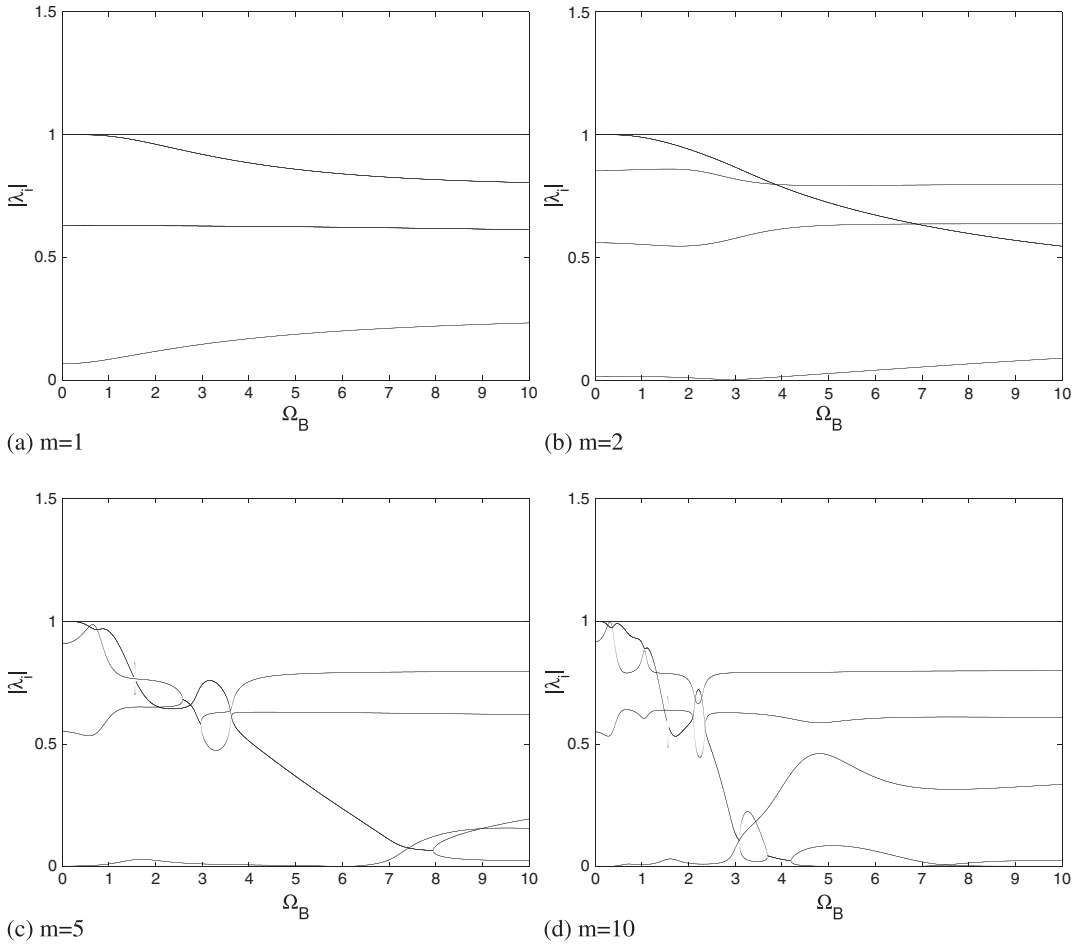

Figure 1. $|\lambda_i|$ of the split oscillator ($b_1 = 1$) for the BGC-macro method: CH-α ($\rho_\infty = 0.8$) coupled with CH-α ($\rho_\infty = 0.5$) with different time step ratios m. (a) $m = 1$; (b) $m = 2$; (c) $m = 5$; (d) $m = 10$.

truncation error depends on the quantity under consideration (displacement, velocity, acceleration, and Lagrange multiplier). In detail, we have

$$\begin{aligned} &\tau_u^A = O\left(h_A^4\right), \tau_v^A = O\left(h_A^3\right), \tau_a^A = O\left(h_A^3\right), \tau_\lambda^A = O\left(h_A^3\right), \\ &\tau_u^B = O\left(h_A^4\right), \tau_v^B = O\left(h_A^3\right), \tau_a^B = O\left(h_A^3\right) \end{aligned} \tag{71}$$

Following the arguments of [132] and [143], a method will be convergent of the order k, if it is stable and consistent of the order k, that is, $\tau_n = O(h_A^{k+1})$. As a result, the BGC-macro HATI is convergent of the order 2 for any time step ratio. The global error plotted in the numerical examples will confirm this numerical analysis. It is important to underline that the second-order accuracy of the α-schemes is preserved through coupling with the BGC-macro method, which is not the case for the algorithms proposed in the literature [143]. Finally, an accurate analysis of the numerical damping ratio and the relative period error can be found in [168] and corroborates the previous truncation error analysis.

As a consequence, the amplification matrix stability analysis of BGC-micro and macro HATI leads to the same stability conclusions as with the pseudo-energy method [132, 143, 168]. Furthermore, it is shown that displacement, velocity, acceleration, and Lagrange multipliers are second-order accurate in the general case for BGC-macro HATI (Equations (67) and (71)). In practice, it is of great interest to scrutinize the possible numerical dissipation coming from the proposed

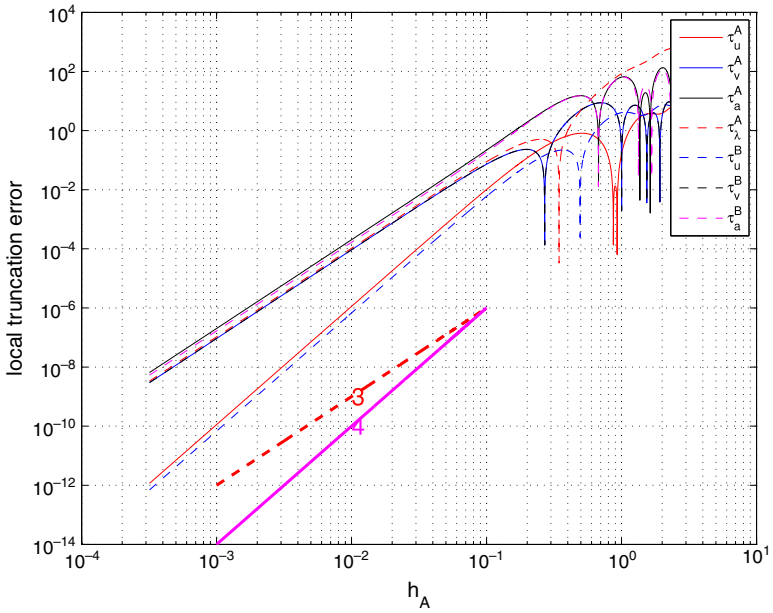

Figure 2. Local truncation error τ of the split oscillator ($b_1 = 1$): CH-α ($\rho_\infty = 0.8$) coupled with CH-α ($\rho_\infty = 0.5$) with time step ratios $m = 2$.

BGC-macro and BGC-micro HATI. Thus, the discrete energy balance equation is detailed in the following in order to estimate the possible numerical damping of the HATI.

3.4. Numerical energy balance for dual HATI

With regard to a given subdomain, the discrete form of the energy balance equation for Newmark time integrators can be found in the works of Hughes [24] and Krenk [111, 118]. Without considering structural damping, the energy balance equation over a time step can be written as

$$\begin{aligned} &\left[\tfrac{1}{2}\dot{\mathbf{u}}^t\mathbf{M}\dot{\mathbf{u}} + \tfrac{1}{2}\mathbf{u}^t\mathbf{K}\mathbf{u} + \left(\beta - \tfrac{\gamma}{2}\right)\tfrac{1}{2}h^2\dot{\mathbf{v}}^t\mathbf{M}\dot{\mathbf{v}}\right]_n^{n+1} = \cdots \\ &\Delta\mathbf{u}^t\left\{\tfrac{1}{2}\left(\mathbf{f}_{n+1} + \mathbf{f}_n\right) + \left(\gamma - \tfrac{1}{2}\right)\left(\mathbf{f}_{n+1} - \mathbf{f}_n\right)\right\} - \left(\gamma - \tfrac{1}{2}\right)\left\{\Delta\mathbf{u}^t\mathbf{K}\Delta\mathbf{u} + \left(\beta - \tfrac{\gamma}{2}\right)h^2\Delta\dot{\mathbf{v}}^t\mathbf{M}\Delta\dot{\mathbf{v}}\right\} \end{aligned} \tag{72}$$

which can also be denoted as

$$\Delta W_{kin} + \Delta W_{int} + \Delta W_{comp} = \Delta W_{ext} + \Delta W_{diss} \tag{73}$$

where ΔW_{kin}, ΔW_{int}, ΔW_{comp}, ΔW_{ext} and ΔW_{diss} are the increments over the time step of the kinetic, internal, complementary, external, and dissipated energies, respectively. The left-hand side of the preceding equation represents the increment of the classical mechanical energy (kinetic plus internal energy) over the time step h, as well as an additional energy, noted here as the complementary energy, coming from the Newmark time integration schemes. The external energy appears on the right-hand side of the balance equation. To study the stability of the algorithm, the external forces can be considered as equal to zero. The stability requires that the left-hand side be definite positive and the right hand side be either equal to zero or negative. In the usual cases of the CAA scheme ($\gamma = \frac{1}{2}$, $\beta = \frac{1}{4}$, second-order accurate) and the CD scheme ($\gamma = \frac{1}{2}$, $\beta = 0$, second-order accurate), it can be easily seen that the right-hand side of Equation (72) is equal to zero, proving that these schemes are non-dissipative. Let us now consider two subdomains Ω_A and Ω_B; the global discrete energy balance equation includes the aforementioned contributions from both subdomains over the macro time step $h_A = [t_0; t_m]$ and over each micro time step $h_B = [t_{j-1}; t_j]$ for j varying from 1 to m, plus an additional term corresponding to the interface energy. The

discrete energy balance equation over the macro time step $h_A = [t_0; t_m]$ for the whole domain can be expressed as

$$\begin{aligned} &\Delta W^A_{kin,m} + \Delta W^A_{int,m} + \Delta W^A_{comp,m} + \sum_{j=1}^{m} \left\{ \Delta W^B_{kin,j} + \Delta W^B_{int,j} + \Delta W^B_{comp,j} \right\} = \dots \\ &\Delta W^A_{ext,m} + \sum_{j=1}^{m} \Delta W^B_{ext,j} + \Delta W^A_{diss,m} + \sum_{j=1}^{m} \Delta W^B_{diss,j} + \Delta W_{interface} \end{aligned} \tag{74}$$

It has been already remarked that the interface forces $\mathbf{L}^t \mathbf{\Lambda}$ act in the same way as the external forces. Thus, the interface energy on the right side of the preceding equation is formed by the contributions from both subdomains:

$$\begin{aligned} \Delta W_{interface} = {} & \Delta \mathbf{u}_m^{A\,t} \left\{ \tfrac{1}{2} \mathbf{L}^t_A \left(\mathbf{\Lambda}_0 + \mathbf{\Lambda}_m \right) + (\gamma_A - \tfrac{1}{2}) \mathbf{L}^t_A \Delta \mathbf{\Lambda}_m \right\} \\ & + \sum_{j=1}^{m} \left\{ \Delta \mathbf{u}_j^{B\,T} \left\{ \tfrac{1}{2} \mathbf{L}^t_B \left(\mathbf{\Lambda}_{j-1} + \mathbf{\Lambda}_j \right) + (\gamma_B - \tfrac{1}{2}) \mathbf{L}^t_B \Delta \mathbf{\Lambda}_j \right\} \right\} \end{aligned} \tag{75}$$

Thus, the interface energy (in the sense of the classical energy norm) can be determined by two ways: either explicitly from Equation (75) or implicitly from Equation (76):

$$\begin{aligned} \Delta W_{interface} = {} & -\Delta W^A_{ext,m} - \sum_{j=1}^{m} \Delta W^B_{ext,j} - \Delta W^A_{diss,m} - \sum_{j=1}^{m} \Delta W^B_{diss,j} \\ & + \Delta W^A_{kin,m} + \Delta W^A_{int,m} + \Delta W^A_{comp,m} + \sum_{j=1}^{m} \left\{ \Delta W^B_{kin,j} + \Delta W^B_{int,j} + \Delta W^B_{comp,j} \right\} \end{aligned} \tag{76}$$

For Newmark time integrators, either Equation (75) or (76) can be used for the numerical estimate of the interface energy (see also (72) for the definition of the energy terms). More generally, for α-schemes, Equation (73) is defined as follows [92]:

$$\begin{aligned} & \left[\tfrac{1}{2} \dot{\mathbf{u}}^t \mathbf{M} \dot{\mathbf{u}} + \tfrac{1}{2} \mathbf{u}^t \mathbf{K} \mathbf{u} + \left(\beta - \tfrac{\gamma}{2} \right) \tfrac{1}{2} h^2 \dot{\mathbf{v}}^t \mathbf{M} \dot{\mathbf{v}} \right]_n^{n+1} = \cdots \\ & \Delta \mathbf{u}^t \left\{ \tfrac{1}{2} \left(\mathbf{f}_{n+1} + \mathbf{f}_n \right) + \left(\gamma - \tfrac{1}{2} \right) \left(\mathbf{f}_{n+1} - \mathbf{f}_n \right) \right\} \\ & \quad - \left(1 - \gamma - \alpha_g \right) \Delta \mathbf{u}^t \mathbf{M} \Delta \dot{\mathbf{v}} - \left(\tfrac{1}{2} - \alpha_f \right) \Delta \mathbf{u}^t \mathbf{K} \Delta \mathbf{u} \\ & \quad - \left(\gamma - \tfrac{1}{2} \right) \left(\beta - \tfrac{\gamma}{2} \right) h^2 \Delta \dot{\mathbf{v}}^t \mathbf{M} \Delta \dot{\mathbf{v}} \end{aligned} \tag{77}$$

Then, for α-schemes, Equation (76) can be used for the numerical estimate of the interface energy with the previous modified definition of the right-hand side. From the aforementioned relationships, it is clear that the standard decreasing energy criterion is not applicable to the class of G-α methods (non-quadratic term on the right-hand side of Equation (77)). Although these methods exhibit growth and decay of the mechanical energy in the linear regime, it is possible to define a norm on the modified state vector $\mathbf{X} \equiv (\mathbf{u}, \dot{\mathbf{u}}, \dot{\mathbf{v}})$ such that $\|\mathbf{X}_{i+1}\| \leqslant \|\mathbf{X}_i\|$ [24, 92]. Thereby, the numerical norm decay of the discrete solution is enough for the G-α schemes to exhibit numerical stability in the linear case. Furthermore, such energy norms can be used as a basis (or a necessary condition) in order to study the stability in the nonlinear regime as suggested, among others, by Belytschko and Shoberle [6, 9, 16, 92].

4. NUMERICAL EXAMPLES

In the following sections, numerical examples are presented to illustrate the properties of the BGC-micro and BGC-macro dual HATI with Newmark and α-schemes. Different time integrators and different timescales are investigated for a SDOF system split into two subdomains. The orders of

accuracy are verified when coupling non-dissipative (Newmark CAA and CD schemes) and dissipative (CH-α, HHT-α, and WBZ -α) schemes, and energetic contributions are scrutinized in both energy norms (pseudo-energy and classical norm of energy). It is recalled that many engineering applications of this method are available in the literature with two or more subdomains with their own integrator and timescale in 2D and 3D (see the state of the art of HATI in Section 3.1 for references). An example with nine subdomains, nine different time integrators, and a maximum ratio of time steps close to 1000 can be found in [145].

4.1. SDOF problem

Generally, for linear structural dynamics simulations, a second-order accuracy is desirable, ensuring that the error of quantities of interest decreases as the square of the time step. To check the order of accuracy of coupling methods, the case of a SDOF oscillator is considered [108, 141]. The oscillator is characterized by its mass and stiffness: $m = 2.10^{-6}$ and $k = 2.10^{4}$. The equilibrium equation of the undamped oscillator under free vibration (no external forces) is given by

$$\dot{v}(t) + \omega^2 u(t) = 0 \tag{78}$$

where $\dot{v}(t)$ and $u(t)$ denote acceleration and displacement, $\omega = \sqrt{\frac{k}{m}}$ being the angular frequency. Initial conditions are prescribed as $u(t=0) = u_0$ and $v(t=0) = v_0$. An initial displacement $u(t=0) = 1$ and a zero initial velocity are taken into account in the following. The mass and the stiffness of the SDOF oscillator are divided into two parts: $m_A = 1.10^{-6}$, $k_A = 1.10^{4}$ and $m_B = 1.10^{-6}$, $k_B = 1.10^{4}$ for the subdomains Ω_A and Ω_B. A Lagrange multiplier is introduced to hold together the two masses. The macro time step h_A is defined on subdomain Ω_A with the CAA implicit Newmark integrator ($\gamma_A = \frac{1}{2}$ and $\beta_A = \frac{1}{4}$). The micro time step h_B is defined on subdomain Ω_B with the CD explicit Newmark integrator ($\gamma_B = \frac{1}{2}$ and $\beta_B = 0$). The ratio between the macro and micro time steps is defined by $m = \frac{h_A}{h_B}$. It is set to 20. The critical time step $h_{B,crit}$ is equal to 2.10^{-5} s. The final time of the free-vibration simulation is $t_f = 2.10^{-4}$ s. The orders of accuracy of the multi-time-step coupling methods are investigated by computing the global error with respect to the analytical solution of the SDOF oscillator in terms of displacements, velocities, and accelerations for the two masses. The reduced angular frequency for the macro subdomain Ω_A is introduced as the product of the angular frequency ω_A with the macro time step h_A: $\Omega_A = \omega_A h_A$. Range of values for the reduced angular frequency Ω_A from 10^{-2} to 10^{-1} is considered for the accuracy order study, corresponding to a macro time step h_A varying from 10^{-7} to 10^{-6} s. The micro time step is less than the critical value $h_{B,crit}$ satisfying the CFL condition [1] for stability requirement of the CD explicit integrator.

4.2. BGC-micro dual HATI

In Figure 3, the BGC-micro method is compared with the GC progenitor method when coupling two non-dissipative second-order accurate Newmark integrators (CAA scheme with CD scheme). The two methods match exactly. The first-order accuracy is obtained for displacement, velocity, and

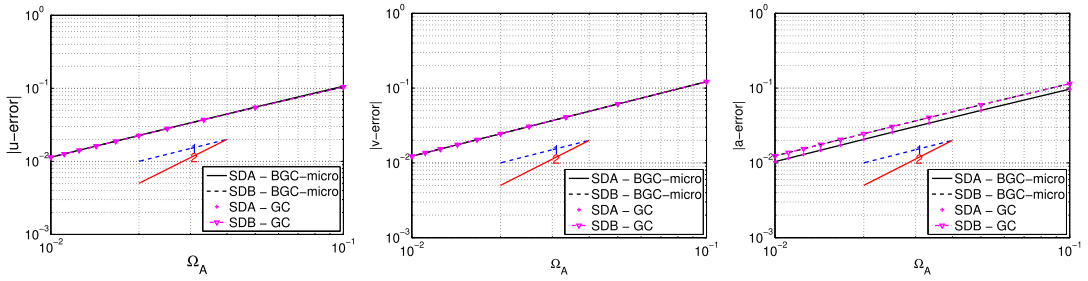

Figure 3. Accuracy orders for the multi-time-step ($m = 20$) BGC-micro and GC (reference) coupling methods for Newmark schemes: CAA ($\gamma_A = \frac{1}{2}$, $\beta_A = \frac{1}{4}$) / CD ($\gamma_B = \frac{1}{2}$, $\beta_B = 0$).

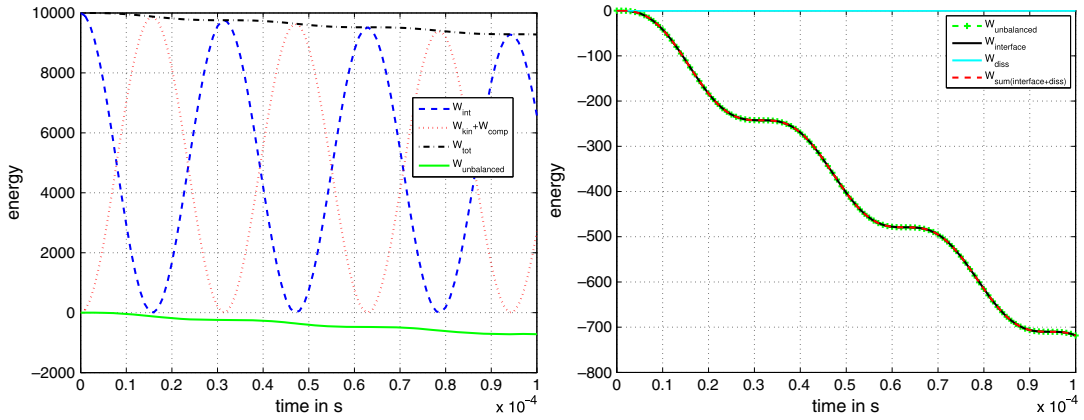

Figure 4. BGC-micro coupling method: CAA $\left(\gamma_A = \frac{1}{2}, \beta_A = \frac{1}{4}\right)$/CD $\left(\gamma_B = \frac{1}{2}, \beta_B = 0\right)$ at $\Omega_A = 10^{-1}$. Discrete energy balance ($m = 20$) and interface energy.

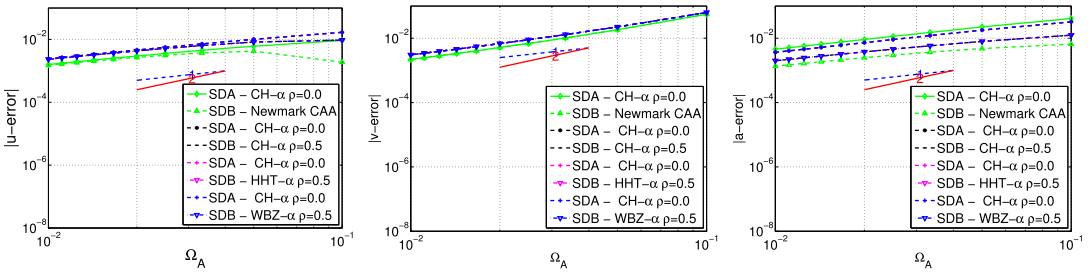

Figure 5. Accuracy orders for the multi-time-step ($m = 20$) BGC-micro coupling method: CH-α ($\rho_\infty = 0.0$)/Newmark (CAA), CH-α ($\rho_\infty = 0.5$), HHT-α ($\rho_\infty = 0.5$), and HHT-α ($\rho_\infty = 0.5$).

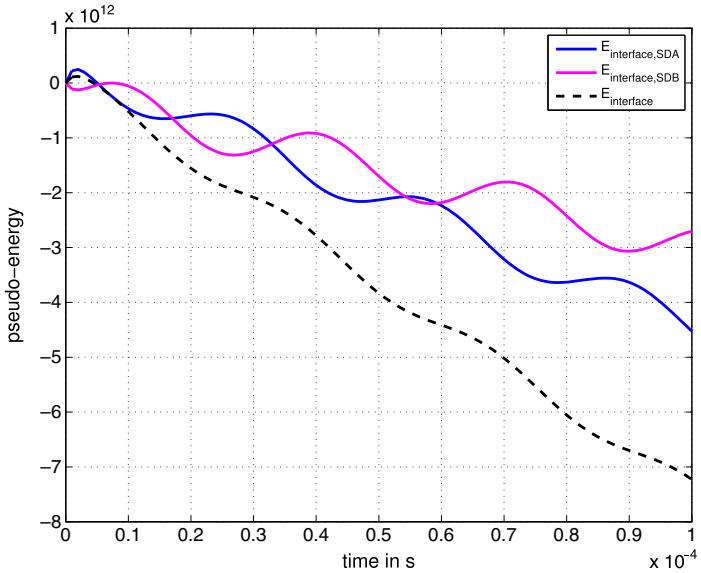

Figure 6. BGC-micro coupling method with $m = 20$: CH-α ($\rho_\infty = 0.0$)/CH-α ($\rho_\infty = 0.5$), at $\Omega_A = 10^{-1}$. Total pseudo-interface energy and contributions from both subdomains.

acceleration, reflecting the energy dissipation characterizing the GC method as soon as different time steps are adopted.

It can be confirmed by Figure 4, which shows the discrete energy balance at the reduced angular frequency Ω_A equal to 10^{-1}. As previously explained, the interface energy $W_{interface}$ is computed in two ways: directly from the Lagrange multipliers from Equation (75) and implicitly from the energy balance in Equation (76) by accounting for all the other energetic contributions. When coupling α-schemes, for example coupling CH-α ($\rho_\infty = 0.0$) related to the first subdomain (macro time step) with Newmark CAA, CH-α, HHT-α, and WBZ-α with the value of ρ_∞ set to 0.5 for the three α-schemes related to the second subdomain (micro time step), the order of accuracy is again equal to 1 for displacement, velocity, and acceleration discretized fields as shown in Figure 5. At the reduced angular frequency $\Omega_A = 10^{-1}$, this dissipative drawback is illustrated by plotting the pseudo-interface energy in Figure 6, along with the contributions from both subdomains according to the expression in Equation (48).

As remarked in Section 3.2.2, the pseudo-interface energy cannot be maintained to the zero value because of the solving of the interface problem at the micro timescale. In Figure 7, the total energy is plotted versus time, corresponding to the sum of internal, kinetic, and complementary energies as written in the left side of the discrete balance equation in Equation (77). The decay of the total energy is observed.

On the basis of this academic example, the consistency, accuracy, and convergence is demonstrated for the proposed BGC-micro dual HATI when dealing with the α-schemes. The dissipative drawback is inherited from the GC progenitor method, leading to the loss of one order of accuracy when we deal with second-order-accurate schemes.

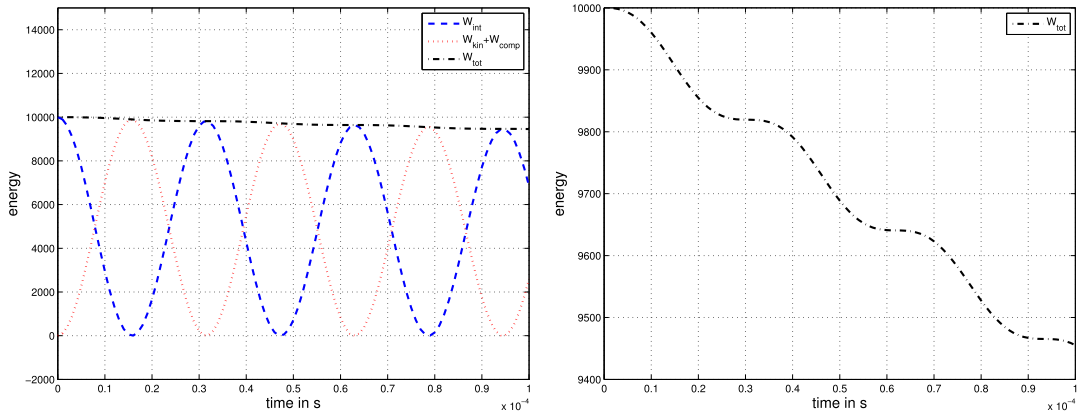

Figure 7. BGC-micro coupling method with $m = 20$: CH-α ($\rho_\infty = 0.0$)/CH-α ($\rho_\infty = 0.5$), at $\Omega_A = 10^{-1}$. Internal, kinetic, and complementary energies ($m = 20$) and total energy.

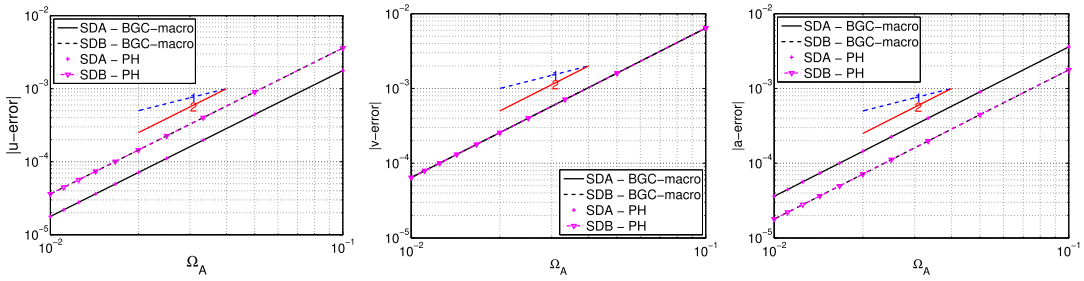

Figure 8. Accuracy orders for the multi-time-step ($m = 20$) BGC-macro and PH (reference) coupling methods for Newmark schemes: CAA $\left(\gamma_A = \frac{1}{2}, \beta_A = \frac{1}{4}\right)$/CD $\left(\gamma_B = \frac{1}{2}, \beta_B = 0\right)$.

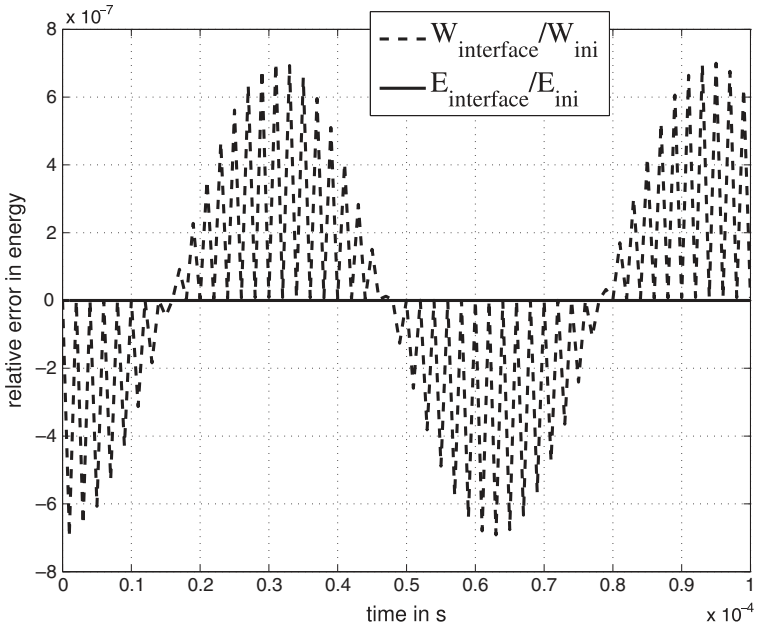

Figure 9. Relative values of interface $W_{interface}$ and pseudo-interface $E_{interface}$ at $\Omega_A = 10^{-1}$ for Newmark schemes: CAA $\left(\gamma_A = \frac{1}{2}, \beta_A = \frac{1}{4}\right)$/CD $\left(\gamma_B = \frac{1}{2}, \beta_B = 0\right)$.

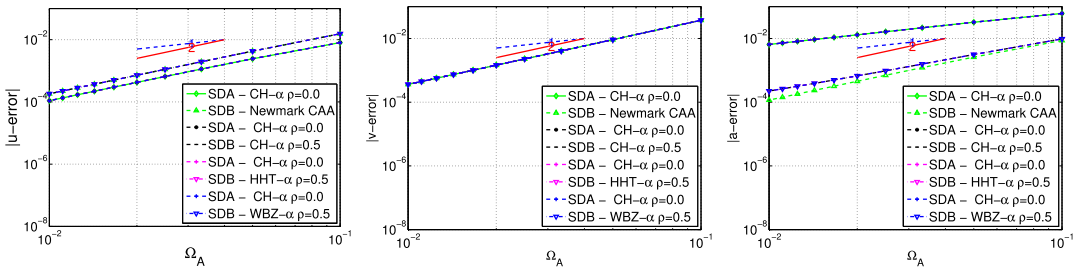

Figure 10. Accuracy orders for the multi-time-step ($m = 20$) BGC-macro coupling method: CH-α ($\rho_\infty = 0.0$)/Newmark (CAA), CH-α ($\rho_\infty = 0.5$), HHT-α ($\rho_\infty = 0.5$), and HHT-α ($\rho_\infty = 0.5$).

4.3. BGC-macro dual HATI

First, the BGC-macro method is compared with the PH method [108] in Figure 8 in the case of non-dissipative second-order-accurate Newmark integrators (CAA scheme with CD scheme). It can be checked that the second-order accuracy in displacement, velocity, and acceleration is maintained through coupling. In the case of Newmark schemes, the BGC-macro method matches exactly the PH method. Because the pseudo-interface energy is chosen as the starting point for building the proposed class of HATI methods, it is important to check that the pseudo-interface energy is equal to zero. From Figure 9 with a reduced angular frequency $\Omega_A = 10^{-1}$, it can be shown that the BGC-macro method preserves the energy in the sense of the energy method: the interface pseudo-energy $E_{interface}$ is exactly equal to 0, whereas the classical norm of the interface energy $W_{interface}$ is very weak (of the order 10^{-7} of the initial internal energy) but is not exactly equal to 0. Secondly, we consider the coupling of α-schemes: CH-α ($\rho_\infty = 0.0$) related to the first subdomain (macro time step) coupled with Newmark CAA, CH-α, HHT-α, and WBZ-α with the value of $\rho_\infty = 0.5$ related to the second subdomain (micro time step). In Figure 10, the order of accuracy of the BGC-macro method is displayed for displacement, velocity, and acceleration. It has to be noted that second-order accuracy is not achieved in acceleration as observed elsewhere [92] for α-schemes. In Figure 11, in the coupling case of CH-α schemes, it can be checked that second-order accuracy is retrieved by apply-

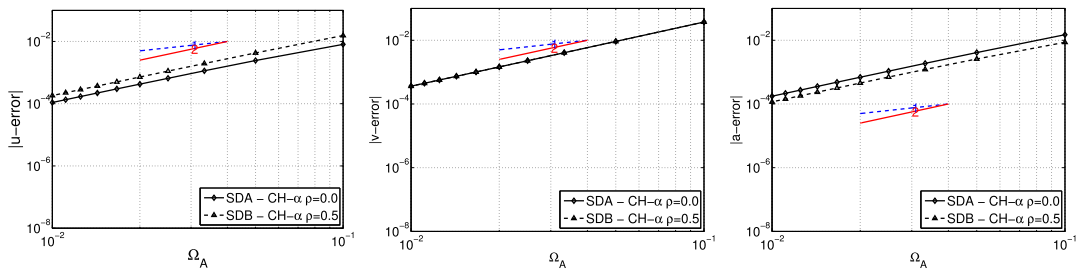

Figure 11. Accuracy orders for the multi-time-step ($m = 20$) BGC-macro coupling method: CH-α ($\rho_\infty = 0.0$)/CH-α ($\rho_\infty = 0.5$) after post-processing of numerical accelerations.

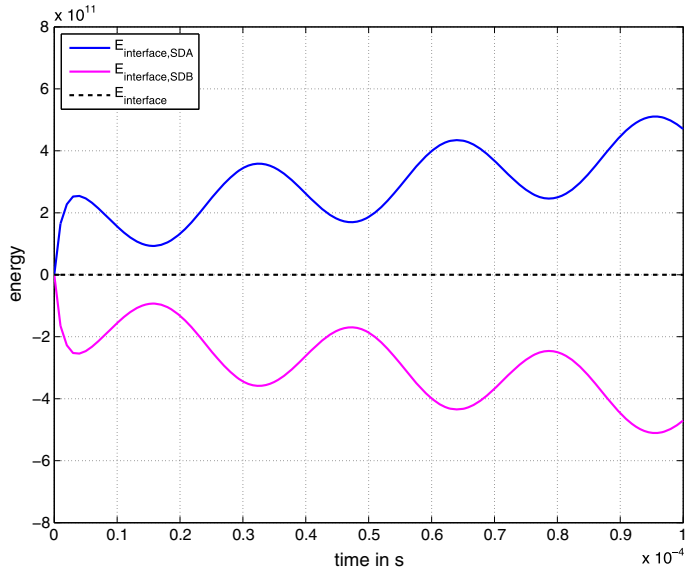

Figure 12. BGC-macro coupling method with $m = 20$: CH-α ($\rho_\infty = 0.0$)/CH-α ($\rho_\infty = 0.5$), at $\Omega_A = 10^{-1}$. Total pseudo-interface energy and contributions from both subdomains.

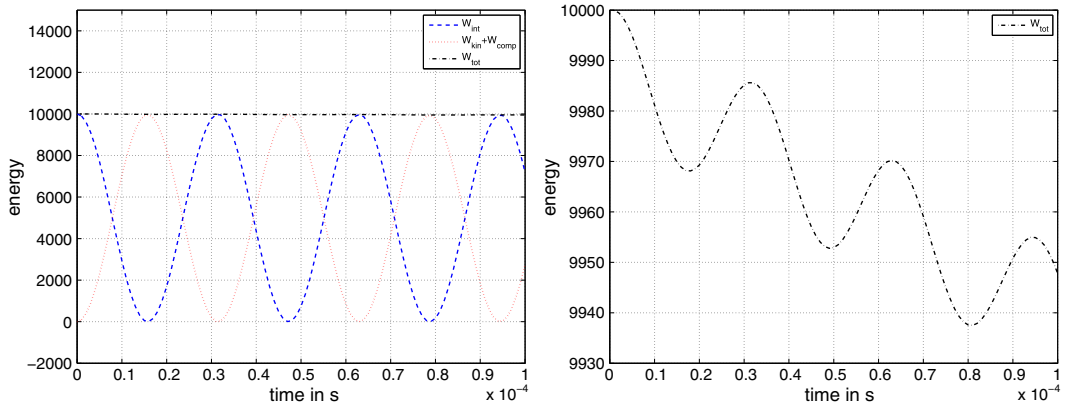

Figure 13. BGC-macro coupling method with $m = 20$: CH-α ($\rho_\infty = 0.0$)/CH-α ($\rho_\infty = 0.5$), at $\Omega_A = 10^{-1}$. Internal, kinetic, and complementary energies ($m = 20$) and total energy.

ing the post-processing procedure concerning the accelerations proposed by Erlicher *et al.* [92]. At an angular frequency $\Omega_A = 10^{-1}$, the pseudo-interface energy is computed from the Lagrange multipliers and plotted in Figure 12 along with the contributions from both subdomains. On the

opposite of the BGC-micro coupling, it can be checked that the BGC-macro dual HATI ensures the zero value of the pseudo-interface. The total energy is plotted versus time in Figure 13 where the growth and decay classically observed for the α-schemes [92] are also obtained. In comparison with the BGC-micro coupling, a less global decay of the total energy is observed, highlighting spurious energy dissipation at the interface coming from the BGC-micro method. Concerning the BGC-macro dual HATI method, it can be concluded that consistency, accuracy, and convergence are well achieved. The energy dissipative drawback of the BGC-micro dual HATI method is alleviated, ensuring the second-order accuracy when dealing with second-order-accurate schemes such as Newmark schemes (CAA and CD) and α-schemes.

5. CONCLUSIONS AND PERSPECTIVES

Based on the pioneer works of Ted Belytschko and coworkers, we have proposed a state of the art on HATI. Historically based on displacement continuity at the interface between heterogenous time integrators, we propose an alternative dual approach based on the velocity continuity. The aim is to build a general methodology for HATI (Newmark, HHT-α, WBZ-α, and CH-α) based on space–time weak formulations and energy considerations. Here, the gluing of subdomains with their own time integrator and their own timescale is ensured with Lagrange multipliers and velocity continuity. Asynchronous kinematic conditions at the interface between the subdomains are obtained by ensuring the zero interface pseudo-energy. Two methods are then derived. The first one (BGC-macro), with velocity continuity at the large timescale, can handle the popular dissipative α-schemes (HHT-α, WBZ-α, and CH-α). In the particular case of Newmark time integrators, the proposed method matches the PH method proposed by Prakash and Hjelmstad in 2004 [108] and also in [163]. The second method (BGC-micro) is based on a velocity gluing at the fine timescale. It can be viewed as an extension to α-schemes of the GC method proposed by Gravouil and Combescure in 2001 [88, 90]. These two families of dual HATI are now popular and applied to a wide range of structural dynamics problems, possibly nonlinear, and also multiphysics, FSI, or general co-simulation strategies. However, BGC-micro approaches remain first-order accurate when second-order time integrators are considered. Developments are in progress to extend BGC-micro approaches at the same level of accuracy as BGC-macro approaches, particularly for strongly nonlinear problems (large strain, frictional contact, non-localized plasticity, etc.). Nevertheless, BGC-micro approaches are still very promising for nonlinear problems owing to their ease of implementation. Furthermore, the extension of dual HATI (macro and micro) to variational integrators has to be studied in detail as the bridge between α-schemes and variational approaches is rather small. Some attempts to use dual HATI to space–time localized multi-grid approaches seem also very interesting when coupled with space–time error indicators [110, 113, 156]. Finally, dual HATI have also been applied recently with success to FSI and co-simulations, and many extensions to multi-physics in general have to be considered.

ACKNOWLEDGEMENTS

We gratefully acknowledge Ted Belytschko for his pioneer and important contributions in HATI.

REFERENCES

1. Courant R, Friedrichs K, Lewy H. Über die partiellen differenzengleichungen der mathematischen physik. *Mathematische Annalen* 1928; **100**(1):32–74.
2. Lax P, Richtmyer R. Survey of the stability of linear finite difference equations. *Communications on Pure and Applied Mathematics* 1956; **9**:267–293.
3. Newmark NM. A method of computation for structural dynamics. *Proceedings of ASCE*, Vol. 85, 1959; 67–94.
4. Dahlquist G. A special stability problem for linear multistep methods. *BIT Numerical Mathematics* 1963; **3**(1):27–43.
5. Washizu K. *Variational Methods in Elasticity and Plasticity*. Pergamon Press, 1975.
6. Belytschko T, Schoeberle D. On the unconditional stability of an implicit algorithm for nonlinear structural dynamics. *Journal of Applied Mechanics* 1975; **42**(4):865–869.

7. Mullen R, Kennedy J, Belytschko T. Application of mesh partitions of explicit–implicit integration to reactor safety problems. *Transactions of the American Nuclear Society 1976 International Meeting*, Vol. 24, Washington, DC, USA, 1976; 275.
8. Belytschko T, Mullen R. Mesh partitions of explicit–implicit time integration. *Formulations and Computational Algorithms in Finite Element Analysis* 1976:673–690.
9. Hughes TJ. Stability, convergence and growth and decay of energy of the average acceleration method in nonlinear structural dynamics. *Computers & Structures* 1976; **6**(4):313–324.
10. Hilber H, Hughes T, Taylor R. Improved numerical dissipation for time integration algorithms in structural dynamics. *Earthquake Engineering and Structural Dynamics* 1977; **5**:283–292.
11. Hughes T, Liu W. Implicit–explicit finite elements in transient analysis: stability theory. *Journal of Applied Mechanics* 1978; **45**:371–374.
12. Belytschko T, Mullen R. Stability of explicit–implicit mesh partitions in time integration. *International Journal for Numerical Methods in Engineering* 1978; **12**(10):1575–1586.
13. Hilber HM, Hughes TJ. Collocation, dissipation and [overshoot] for time integration schemes in structural dynamics. *Earthquake Engineering & Structural Dynamics* 1978; **6**(1):99–117.
14. Hughes T, Pister K, Taylor R. Implicit–explicit finite elements in nonlinear transient analysis. *Computer Methods in Applied Mechanics and Engineering* 1979; **17/18**:159–182.
15. Belytschko T, Yen H, Mullen R. Mixed methods for time integration. *Computer Methods in Applied Mechanics and Engineering* 1979; **17**(18):259–275.
16. Wood W, Bossak M, Zienkiewicz O. An alpha modification of Newmark's method. *International Journal for Numerical Methods in Engineering* 1980; **15**(10):1562–1566.
17. Park K. Partitioned transient analysis procedures for coupled-field problems: stability analysis. *Journal of Applied Mechanics* 1980; **47**:370.
18. Liu W, Belytschko T. Mixed-time implicit–explicit finite elements for transient analysis. *Computers and Structures* 1982; **15**:445–450.
19. Underwood P, Belytschko T, Hughes TJR. *Computational Methods for Transient Analysis* T. Belytschko, TJR Hughes (eds). Elsevier Science Publishers, 1983, 245–265.
20. Zienkiewicz O, Wodd W, Hine N, Taylor R. A unified set of single step algorithms. I: general formulation and applications. *International Journal for Numerical Methods in Engineering* 1984; **20**(8):1529–1552.
21. Belytschko T, Smolinski P, Liu W. Stability of multi-time step partitioned integrators for first-order finite element systems. *Computer Methods in Applied Mechanics and Engineering* 1985; **49**:281–297.
22. Ortiz M. A note on energy conservation and stability of nonlinear time-stepping algorithms. *Computers & Structures* 1986; **24**(1):167–168.
23. Guennouni T, Aubry D. Reponse homogénéisée en temps de structures sous chargements cycliques. *Comptes rendus de l'Académie des sciences. Série 2, Mécanique, Physique, Chimie, Sciences de l'univers, Sciences de la Terre* 1986; **303**(20):1765–1768.
24. Hughes T. *The Finite Element Method: Linear Static and Dynamic Finite Element Analysis*. Prentice-Hall: Englewood Cliffs, NJ, 1987.
25. Hulbert G, Hughes T. An error analysis of truncated starting conditions in step-by-step time integration: consequences for structural dynamics. *Earthquake Engineering & Structural Dynamics* 1987; **15**(7):901–910.
26. Smolinski P, Belytschko T, Neal M. Multi-time-step integration using nodal partitioning. *International Journal for Numerical Methods in Engineering* 1988; **26**:349–359.
27. Hughes T, Hulbert G. Space–time finite element methods for elastodynamics: formulations and error estimates. *Computer Methods in Applied Mechanics and Engineering* 1988; **66**(3):339–363.
28. Belytschko T, Liu W, Engelmann B. A review of recent developments in time integration. *State-of-the-art surveys on computational mechanics(A 90-47176 21-64). New York, American Society of Mechanical Engineers, 1989* 1989:185–199.
29. Cardona A, Geradin M. Time integration of the equations of motion in mechanism analysis. *Computers & Structures* 1989; **33**(3):801–820.
30. Roux F. Méthodes de résolution par sous-domaines en statique. *La Recherche Aérospatiale* 1990; **1**:37–48.
31. Wood W. *Practical Time-stepping Schemes*. Clarendon Press: Oxford [England], 1990.
32. Hulbert G, Hughes T. Space–time finite element methods for second-order hyperbolic equations. *Computer Methods in Applied Mechanics and Engineering* 1990; **84**(3):327–348.
33. Farhat C, Roux F. A method of finite element tearing and interconnecting and its parallel solution algorithm. *International Journal for Numerical Methods in Engineering* 1991; **32**(6):1205–1227.
34. Simo JC, Wong KK. Unconditionally stable algorithms for rigid body dynamics that exactly preserve energy and momentum. *International Journal for Numerical Methods in Engineering* 1991; **31**(1):19–52.
35. Zienkiewicz O, Taylor R. *The Finite Element Method* (4th edn), Solid and Fluid Mechanics/Dynamics and Non-Linearity, vol. 2. McGraw-Hill: New York, 1991.
36. Wiberg N, Zeng L, Li X. Error estimation and adaptivity in elastodynamics. *Computer Methods in Applied Mechanics and Engineering* 1992; **101**(1–3):369–395.
37. Simo J, Tarnow N. The discrete energy-momentum method. conserving algorithms for nonlinear elastodynamics. *Zeitschrift für Angewandte Mathematik und Physik (ZAMP)* 1992; **43**(5):757–792.
38. Smolinski P. An explicit multi-time step integration method for second order equations. *Computer Methods in Applied Mechanics and Engineering* 1992; **94**:25–34.

39. Smolinski P. Stability analysis of multi-time step explicit integration method. *Computer Methods in Applied Mechanics and Engineering* 1992; **95**:291–300.
40. Simo J, Tarnow N, Wong K. Exact energy-momentum conserving algorithms and symplectic schemes for nonlinear dynamics. *Computer Methods in Applied Mechanics and Engineering* 1992; **100**(1):63–116.
41. Hulbert G. Time finite element methods for structural dynamics. *International Journal for Numerical Methods in Engineering* 1992; **33**:307–331.
42. Belytschko T, Lu Y. Stability analysis of elemental explicit–implicit partitions by Fourier methods. *Computer Methods in Applied Mechanics and Engineering* 1992; **95**:87–96.
43. Belytschko T, Lu Y. Explicit multi-time step integration for first and second order finite element semidiscretizations. *Computer Methods in Applied Mechanics and Engineering* 1993; **108**:353–383.
44. Safjan A, Oden J. High-order Taylor–Galerkin and adaptive h–p methods for second-order hyperbolic systems: application to elastodynamics. *Computer Methods in Applied Mechanics and Engineering* 1993; **103**(1–2):187–230.
45. Chung J, Hulbert G. A time integration algorithm for structural dynamics with improved numerical dissipation: the generalized-α method. *Journal of Applied Mechanics* 1993; **60**(2):371–375.
46. Farhat C, Crivelli L, Roux F. A transient FETI methodology for large-scale parallel implicit computations in structural mechanics. *International Journal for Numerical Methods in Engineering* 1994; **37**(11):1945–1975.
47. Richter G. An explicit finite element method for the wave equation. *Applied Numerical Mathematics* 1994; **16**(1–2):65–80.
48. Chung J, Hulbert GM. A family of single-step Houbolt time integration algorithms for structural dynamics. *Computer Methods in Applied Mechanics and Engineering* 1994; **118**(1):1–11.
49. Sotelino E. A concurrent explicit–implicit algorithm in structural dynamics. *Computers & Structures* 1994; **51**(2):181–190.
50. Farhat C, Crivelli L, Géradin M. Implicit time integration of a class of constrained hybrid formulations. Part I: spectral stability theory. *Computer Methods in Applied Mechanics and Engineering* 1995; **125**(1):71–107.
51. Bauchau O, Damilano G, Theron N. Numerical integration of non-linear elastic multi-body systems. *International Journal for Numerical Methods in Engineering* 1995; **38**(16):2727–2751.
52. Piché R. An l-stable Rosenbrock method for step-by-step time integration in structural dynamics. *Computer Methods in Applied Mechanics and Engineering* 1995; **126**(3):343–354.
53. Cho J, Youn S. A hierarchical time adaptive refinement scheme for the finite element elastodynamics. *Computers and Structures* 1995; **56**(4):645–650.
54. Cannarozzi M, Mancuso M. Formulation and analysis of variational methods for time integration of linear elastodynamics. *Computer Methods in Applied Mechanics and Engineering* 1995; **127**(1):241–257.
55. Smolinski P, Sleith S, Belytschko T. Stability of an explicit multi-time step integration algorithm for linear structural dynamics equations. *Computational Mechanics* 1996; **18**(3):236–244.
56. Hulbert G, Chung J. Explicit time integration algorithms for structural dynamics with optimal numerical dissipation. *Computer Methods in Applied Mechanics and Engineering* 1996; **137**(2):175–188.
57. Geradin M, Rixen D. *Mechanical Vibrations: Theory and Application to Structural Dynamics*, Vol. 25. John Wiley: New York, 1997.
58. Laursen T, Chawla V. Design of energy conserving algorithms for frictionless dynamic contact problems. *International Journal for Numerical Methods in Engineering* 1997; **40**(5):863–886.
59. Daniel W. Analysis and implementation of a new constant acceleration subcycling algorithm. *International Journal for Numerical Methods in Engineering* 1997; **37**:2841–2855.
60. Combescure D, Pegon P. α-Operator splitting time integration technique for pseudodynamic testing—error propagation analysis. *Soil Dynamics and Earthquake Engineering* 1997; **16**:427–443.
61. Daniel W. The subcycled Newmark algorithm. *Computational Mechanics* 1997; **20**(3):272–281.
62. Daniel W. A study of the stability of subcycling algorithms in structural dynamics. *Computer Methods in Applied Mechanics and Engineering* 1998; **156**:1–13.
63. Daniel W. Subcycling first- and second-order generalizations of the trapezoidal rule. *International Journal for Numerical Methods in Engineering* 1998; **42**:1091–1119.
64. Klisinski M, Mostrom A. On stability of multitime step integration procedures. *Journal of Engineering Mechanics* 1998; **124**(7):783–793.
65. Armero F, Petocz E. Formulation and analysis of conserving algorithms for frictionless dynamic contact/impact problems. *Computer Methods in Applied Mechanics and Engineering* 1998; **158**(3):269–300.
66. Combescure A, Gayffier A, Gravouil A, Greffet N. A lagrange multiplier based domain decomposition method for time-dependent problems involving several time-scales. *IV World Congress on Computational Mechanics, Buenos Aires*, 1998.
67. Smolinski P, Wu Y. Stability of explicit subcycling time integration with linear interpolation for first-order finite element semidiscretizations. *Computer Methods in Applied Mechanics and Engineering* 1998; **151**:311–324.
68. Farhat C, Lesoinne M, Le Tallec P. Load and motion transfer algorithms for fluid/structure interaction problems with non-matching discrete interfaces: momentum and energy conservation, optimal discretization and application to aeroelasticity. *Computer Methods in Applied Mechanics and Engineering* 1998; **157**(1):95–114.
69. Kuhl D, Crisfield M. Energy-conserving and decaying algorithms in non-linear structural dynamics. *International Journal for Numerical Methods in Engineering* 1999; **45**(5):569–599.
70. Moreau JJ. Numerical aspects of the sweeping process. *Computer Methods in Applied Mechanics and Engineering* 1999; **177**(3):329–349.

71. Jean M. The non-smooth contact dynamics method. *Computer Methods in Applied Mechanics and Engineering* 1999; **177**(3):235–257.
72. Wiberg N, Li X. Adaptive finite element procedures for linear and non-linear dynamics. *International Journal for Numerical Methods in Engineering* 1999; **46**(10):1781–1802.
73. Park K, Felippa CA. A variational principle for the formulation of partitioned structural systems. *International Journal for Numerical Methods in Engineering* 2000; **47**(1-3):395–418.
74. Gravouil A, Combescure A. Méthode multi-chelles en temps et en espace avec dcomposition de domaines pour la dynamique non-linaire des structures. *Ph.D. Thesis*, École normale supérieure de Cachan-ENS Cachan, 2000, 229 pages.
75. Nawrotzki P, Eller C. Numerical stability analysis in structural dynamics. *Computer Methods in Applied Mechanics and Engineering* 2000; **189**(3):915–929.
76. Schleupen A, Ramm E. Local and global error estimations in linear structural dynamics. *Computers and Structures* 2000; **76**(6):741–756.
77. Yin L, Acharya A, Sobh N, Haber R, Tortorelli D, Cockburn B, Karniadakis G, Shu C. *Discontinuous Galerkin Methods: Theory, Computation and Applications 11*. Springer: Berlin, 2000.
78. Wu Y, Smolinski P. A multi-time step integration algorithm for structural dynamics based on the modified trapezoidal rule. *Computer Methods in Applied Mechanics and Engineering* 2000; **187**:641–660.
79. Combescure A, Gravouil A. A time–space multi-scale algorithm for transient structural nonlinear problems. *Mecanique & Industries* 2001; **2**(1):43–55.
80. Felippa CA, Park K, Farhat C. Partitioned analysis of coupled mechanical systems. *Computer Methods in Applied Mechanics and Engineering* 2001; **190**(24):3247–3270.
81. Piperno S, Farhat C. Partitioned procedures for the transient solution of coupled aeroelastic problems—part II: energy transfer analysis and three-dimensional applications. *Computer Methods in Applied Mechanics and Engineering* 2001; **190**(24-25):3147–3170.
82. Czekanski A, El-Abbasi N, Meguid S. Optimal time integration parameters for elastodynamic contact problems. *Communications in Numerical Methods in Engineering* 2001; **17**(6):379–384.
83. Armero F, Romero I. On the formulation of high-frequency dissipative time-stepping algorithms for nonlinear dynamics. Part I: low-order methods for two model problems and nonlinear elastodynamics. *Computer Methods in Applied Mechanics and Engineering* 2001; **190**(20–21):2603–2649.
84. Armero F, Romero I. On the formulation of high-frequency dissipative time-stepping algorithms for nonlinear dynamics. Part II: second-order methods. *Computer Methods in Applied Mechanics and Engineering* 2001; **190**(51–52):6783–6824.
85. Marsden JE, West M. Discrete mechanics and variational integrators. *Acta Numerica* 2001; **10**(1):357–514.
86. Bottasso CL, Borri M, Trainelli L. Integration of elastic multibody systems by invariant conserving/dissipating algorithms. II. Numerical schemes and applications. *Computer Methods in Applied Mechanics and Engineering* 2001; **190**(29):3701–3733.
87. Pegon P. Alternative characterization of time integration schemes. *Computer Methods in Applied Mechanics and Engineering* 2001; **190**(20):2707–2727.
88. Gravouil A, Combescure A. Multi-time-step explicit–implicit method for non-linear structural dynamics. *International Journal for Numerical Methods in Engineering* 2001; **50**:199–225.
89. Betsch P, Steinmann P. Conservation properties of a time FE method–part ii: time-stepping schemes for non-linear elastodynamics. *International Journal for Numerical Methods in Engineering* 2001; **50**(8):1931–1955.
90. Combescure A, Gravouil A. A numerical scheme to couple subdomains with different time-steps for predominantly linear transient analysis. *Computer Methods in Applied Mechanics and Engineering* 2002; **191**(11–12):1129–1157.
91. Pandolfi A, Kane C, Marsden J, Ortiz M. Time-discretized variational formulation of non-smooth frictional contact. *International Journal for Numerical Methods in Engineering* 2002; **53**(8):1801–1829.
92. Erlicher S, Bonaventura L, Bursi O. The analysis of the generalized-α method for non-linear dynamic problems. *Computational Mechanics* 2002; **28**(2):83–104.
93. Herry B, Di Valentin L, Combescure A. An approach to the connection between subdomains with non-matching meshes for transient mechanical analysis. *International Journal for Numerical Methods in Engineering* 2002; **55**:973–1003.
94. Gravouil A, Combescure A. Multi-time-step and two-scale domain decomposition method for non-linear structural dynamics. *International Journal for Numerical Methods in Engineering* 2003; **58**:1545–1569.
95. Michler C, Van Brummelen E, Hulshoff S, De Borst R. The relevance of conservation for stability and accuracy of numerical methods for fluid–structure interaction. *Computer Methods in Applied Mechanics and Engineering* 2003; **192**(37):4195–4215.
96. Combescure A, Gravouil A, Herry B. An algorithm to solve transient structural non-linear problems for non-matching time–space domains. *Computers and Structures* 2003; **81**(12):1211–1222.
97. Faucher V, Combescure A. A time and space mortar method for coupling linear modal subdomains and non-linear subdomains in explicit structural dynamics. *Computer Methods in Applied Mechanics and Engineering* 2003; **192**(5):509–533.
98. Kanapady R, Tamma K. On a novel design of a new unified variational framework of discontinuous/continuous time operators of high order and equivalence. *Finite Elements in Analysis and Design* 2003; **39**(8):727–749.
99. Daniel W. Explicit/implicit partitioning and a new explicit form of the generalized alpha method. *Communications in Numerical Methods in Engineering* 2003; **19**(11):909–920.

100. Daniel W. A partial velocity approach to subcycling structural dynamics. *Computer Methods in Applied Mechanics and Engineering* 2003; **192**(3):375–394.
101. Lew A, Marsden JE, Ortiz M, West M. Asynchronous variational integrators. *Archive for Rational Mechanics and Analysis* 2003; **167**(2):85–146.
102. Hulbert GM. *Computational Structural Dynamics*. Wiley Online Library, 2004.
103. Faucher V, Combescure A. Local modal reduction in explicit dynamics with domain decomposition. Part 1: extension to subdomains undergoing finite rigid rotations. *International Journal for Numerical Methods in Engineering* 2004; **60**:2531–2560.
104. Faucher V, Combescure A. Local modal reduction in explicit dynamics with domain decomposition. Part 2: specific interface treatment when modal subdomains are involved. *International Journal for Numerical Methods in Engineering* 2004; **61**:69–95.
105. Noels L, Stainier L, Ponthot JP. Combined implicit/explicit algorithms for crashworthiness analysis. *International Journal of Impact Engineering* 2004; **30**(8):1161–1177.
106. Noels L, Stainier L, Ponthot JP. Combined implicit/explicit time-integration algorithms for the numerical simulation of sheet metal forming. *Journal of Computational and Applied Mathematics* 2004; **168**(1):331–339.
107. Pinto A, Pegon P, Magonette G, Tsionis G. Pseudo-dynamic testing of bridges using non-linear substructuring. *Earthquake Engineering and Structural Dynamics* 2004; **33**:1125–1146.
108. Prakash A, Hjelmstad K. A FETI-based multi-time-step coupling method for Newmark schemes in structural dynamics. *International Journal for Numerical Methods in Engineering* 2004; **61**(13):2183–2204.
109. Palaniappan J, Haber R, Jerrard R. A space–time discontinuous Galerkin method for scalar conservation laws. *Computer Methods in Applied Mechanics and Engineering* 2004; **193**:3607–3631.
110. Abedi R, Zhou Y, Chung S, Erickson J, Fan Y, Garland M, Guoy D, Haber R, Sullivan J, Thite S. Space–time meshing with adaptive refinement and coarsening. *Proceedings of the Twentieth Annual Symposium on Computational Geometry*, 2004; 300–309.
111. Krenk S, Høgsberg J. Properties of time integration with first order filter damping. *International Journal for Numerical Methods in Engineering* 2005; **64**:547–566.
112. Réthoré J, Gravouil A, Combescure A. A combined space–time extended finite element method. *International Journal for Numerical Methods in Engineering* 2005; **64**:260–284.
113. Cavin P, Gravouil A, Lubrecht A, Combescure A. Automatic energy conserving space–time refinement for linear dynamic structural problems. *International Journal for Numerical Methods in Engineering* 2005; **64**:304–321.
114. Abedi R, Petracovici B, Haber R. A space–time discontinuous Galerkin method for linearized elastodynamics with element-wise momentum balance. *Computer Methods in Applied Mechanics and Engineering* 2005; **195**(25–28):3247–3273.
115. Farhat C, van der Zee KG, Geuzaine P. Provably second-order time-accurate loosely-coupled solution algorithms for transient nonlinear computational aeroelasticity. *Computer Methods in Applied Mechanics and Engineering* 2006; **195**(17):1973–2001.
116. Bourel B, Combescure A, Di Valentin L. Handling contact in multi-domain simulation of automobile crashes. *Finite Elements in Analysis and Design* 2006; **42**(8):766–779.
117. Abedi R, Haber R, Thite S, Erickson J. An h-adaptive space time-discontinuous Galerkin method for linearized elastodynamics. *Revue Européenne des Eléments Finis* 2006; **15/6**:619–642.
118. Krenk S. Energy conservation in Newmark based time integration algorithms. *Computer Methods in Applied Mechanics and Engineering* 2006; **195**(44–47):6110–6124.
119. Hauret P, Le Tallec P. Energy-controlling time integration methods for nonlinear elastodynamics and low-velocity impact. *Computer Methods in Applied Mechanics and Engineering* 2006; **195**(37):4890–4916.
120. Krenk S. State–space time integration with energy control and fourth-order accuracy for linear dynamic systems. *International Journal for Numerical Methods in Engineering* 2006; **65**(5):595–619.
121. Chen W, Fish J. A generalized space–time mathematical homogenization theory for bridging atomistic and continuum scales. *International Journal for Numerical Methods in Engineering* 2006; **67**(2):253–271.
122. Arnold M, Bruls O. Convergence of the generalized-α scheme for constraint mechanical systems. *Multibody System Dynamics* 2007; **18**:185–202.
123. Magoules F, Roux FX and others. Algorithms and theory of substructuring and domain decomposition methods. *Mesh Partitioning Techniques and Domain Decomposition Methods* 2007:89–118.
124. van Zuijlen A, Bosscher S, Bijl H. Two level algorithms for partitioned fluid–structure interaction computations. *Computer Methods in Applied Mechanics and Engineering* 2007; **196**(8):1458–1470.
125. Krenk S. The role of geometric stiffness in momentum and energy conserving time integration. *International Journal for Numerical Methods in Engineering* 2007; **71**(6):631–651.
126. Kale KG, Lew AJ. Parallel asynchronous variational integrators. *International Journal for Numerical Methods in Engineering* 2007; **70**(3):291–321.
127. Focardi M, Mariano PM. Convergence of asynchronous variational integrators in linear elastodynamics. *International Journal for Numerical Methods in Engineering* 2008; **75**(7):755–769.
128. BenDhia H. Further insights by theoretical investigations of the multiscale Arlequin method. *International Journal of Multiscale Comparative Engineering* 2008; **6**:215–232.
129. Fong W, Darve E, Lew A. Stability of asynchronous variational integrators. *Journal of Computational Physics* 2008; **227**(18):8367–8394.

130. Krenk S. Extended state-space time integration with high-frequency energy dissipation. *International Journal for Numerical Methods in Engineering* 2008; **73**(12):1767–1787.
131. Bonnet P, Williams M, Blakeborough A. Evaluation of numerical time-integration schemes for real-time hybrid testing. *Earthquake Engineering and Structural Dynamics 2008* 2008; **37**:1467–1490.
132. Bonelli A, Bursi O, He L, Magonette G, Pegon P. Convergence analysis of a parallel interfield method for heterogeneous simulations with dynamic substructuring. *International Journal for Numerical Methods in Engineering* 2008; **75**:800–825.
133. Hoitink A, Masuri S, Zhou X, Tamma K. Algorithms by design: part i on the hidden point collocation within LMS methods and implications for nonlinear dynamics applications. *International Journal for Computational Methods in Engineering Science and Mechanics* 2008; **9**(6):383–407.
134. Casadei T, Halleux J. Binary spatial partitioning of the central-difference time integration scheme for explicit fast transient dynamics. *International Journal for Numerical Methods in Engineering* 2009; **78**:1436–1473.
135. Masuri S, Hoitink A, Zhou X, Tamma K. Algorithms by design: part III. A novel normalized time weighted residual methodology and design of optimal symplectic-momentum based controllable numerical dissipative algorithms for nonlinear structural dynamics. *International Journal for Computational Methods in Engineering Science and Mechanics* 2009; **10**(1):57–90.
136. Aubertin P, Réthoré J, DeBorst R. Energy conservation of atomistic/continuum coupling. *International Journal for Numerical Methods in Engineering* 2009; **78**:1365–1386.
137. Masuri S, Hoitink A, Zhou X, Tamma K. Algorithms by design: part II. A novel normalized time weighted residual methodology and design of a family of symplectic-momentum conserving algorithms for nonlinear structural dynamics. *International Journal for Computational Methods in Engineering Science and Mechanics* 2009; **10**(1):27–56.
138. Romero I. Thermodynamically consistent time-stepping algorithms for non-linear thermomechanical systems. *International Journal for Numerical Methods in Engineering* 2009; **79**(6):706–732.
139. Masuri S, Hoitink A, Zhou X, Tamma K. Algorithms by design: a new normalized time-weighted residual methodology and design of a family of energy-momentum conversing algorithms for non-linear structural dynamics. *International Journal for Numerical Methods in Engineering* 2009; **79**:1094–1146.
140. Mahjoubi N, Gravouil A, Combescure A. Coupling subdomains with heterogeneous time integrators and incompatible time steps. *Computational Mechanics* 2009; **44**(6):825–843.
141. Mahjoubi N, Krenk S. Multi-time-step domain coupling method with energy control. *International Journal for Numerical Methods in Engineering* 2010; **83**(13):1700–1718.
142. Mahjoubi N. Méthode générale de couplage de schéma d'intégration multi-échelles en temps en dynamique des structures. *Ph.D. Thesis*, Institut National des Sciences Appliquées de LYON, 2010.
143. Bursi O, He L, Bonelli A, Pegon P. Novel generalized-α methods for interfield parallel integration of heterogeneous structural dynamic systems. *Journal of Computational and Applied Mathematics* 2010; **234**:2250–2258.
144. Beneš M, Matouš K. Asynchronous multi-domain variational integrators for nonlinear hyperelastic solids. *Computer Methods in Applied Mechanics and Engineering* 2010; **199**(29):1992–2013.
145. Mahjoubi N, Gravouil A, Combescure A, Greffet N. A monolithic energy conserving method to couple heterogeneous time integrators with incompatible time steps in structural dynamics. *Computer Methods in Applied Mechanics and Engineering* 2011; **200**:1069–1086.
146. Chhay M, Hamdouni A. On the accuracy of invariant numerical schemes. *Communications on Pure and Applied Analysis* 2011; **10**(2):761–783.
147. Chhay M, Hoarau E, Hamdouni A, Sagaut P. Comparison of some lie-symmetry-based integrators. *Journal of Computational Physics* 2011; **230**(5):2174–2188.
148. Abaqus 6.13. analysis users guide: co-simulation section 17.1. Substructuring, section 10.1. Abaqus technology brief: full vehicle durability using Abaqus/standard to Abaqus/explicit co-simulation, 2011.
149. Batti A, Brun M, Combescure A, Gravouil A, *et al.* Comparaison de codes externes de couplage basés sur quatre méthodes de décomposition de sous domaines. *10e Colloque National en Calcul des Structures*, 2011.
150. Brun M, Batti A, Limam A, Combescure A. Implicit/explicit multi-time step co-computations for predicting reinforced concrete structure response under earthquake loading. *Soil Dynamics and Earthquake Engineering* 2012; **33**(1):19–37.
151. Brun M, Batti A, Limam A, Gravouil A. Explicit/implicit multi-time step co-computations for blast analyses on a reinforced concrete frame structure. *Finite Elements in Analysis & Design* 2012; **52**:41–59.
152. Ghanem A, Torkhani M, Mahjoubi N, Baranger T, Combescure A. Arlequin framework for multi-model, multi-time scale and heterogeneous time integrators for structural transient dynamics. *Computer Methods in Applied Mechanics and Engineering* 2012.
153. Ryckman RA, Lew AJ. An explicit asynchronous contact algorithm for elastic body–rigid wall interaction. *International Journal for Numerical Methods in Engineering* 2012; **89**(7):869–896.
154. Confalonieri F, Cocchetti G, Ghisi A, Corigliano A. A domain decomposition method for the simulation of fracture in polysilicon MEMS. *2012 13th International Conference on Thermal, Mechanical and Multi-physics Simulation and Experiments in Microelectronics and Microsystems (EuroSimE),* IEEE, 2012; 1–8.
155. González JA, Park K. A simple explicit–implicit finite element tearing and interconnecting transient analysis algorithm. *International Journal for Numerical Methods in Engineering* 2012; **89**(10):1203–1226.
156. Biotteau E, Gravouil A, Lubrecht AA, Combescure A. Three dimensional automatic refinement method for transient small strain elastoplastic finite element computations. *Computational Mechanics* 2012; **49**:123–136.

157. Corigliano A, Dossi M, Mariani S. Recent advances in computational methods for microsystems. *Advanced Materials Research* 2013; **745**:13–25.
158. Bettinotti O, Allix O, Malherbe B. A coupling strategy for adaptive local refinement in space and time with a fixed global model in explicit dynamics. *Computational Mechanics* 2013:1–14.
159. Ghanem A, Torkhani M, Mahjoubi N, Baranger T, Combescure A. Arlequin framework for multi-model, multi-time scale and heterogeneous time integrators for structural transient dynamics. *Computer Methods in Applied Mechanics and Engineering* 2013; **254**:292–308.
160. Confalonieri F, Corigliano A, Dossi M, Gornati M. A domain decomposition technique applied to the solution of the coupled electro-mechanical problem. *International Journal for Numerical Methods in Engineering* 2013; **93**(2): 137–159.
161. Li Z, Combescure A, Leboeuf F. Coupling of finite volume and finite element subdomains using different time integrators. *International Journal for Numerical Methods in Fluids* 2013; **72**(12):1286–1306.
162. Boucinha L, Gravouil A, Ammar A. Space–time proper generalized decompositions for the resolution of transient elastodynamic models. *Computer Methods in Applied Mechanics and Engineering* 2013; **255**:67–88.
163. Karimi S, Nakshatrala K. On multi-time-step monolithic coupling algorithms for elastodynamics. *Journal of Computational Physics* 2014; **273**:671–705.
164. Brun M, Batti A, Combescure A, Gravouil A. External coupling software based on macro- and micro-time scales for explicit/implicit multi-time-step co-computations in structural dynamics. *Finite Elements in Analysis and Design* 2014; **86**:101–119.
165. Ibrahimbegovic A, Niekamp R, Kassiotis C, Markovic D, Matthies HG. Code-coupling strategy for efficient development of computer software in multiscale and multiphysics nonlinear evolution problems in computational mechanics. *Advances in Engineering Software,* Elsevier 2014; **72**:8–17.
166. Chantrait T, Rannou J, Gravouil A. Low intrusive coupling of implicit and explicit time integration schemes for structural dynamics: application to low energy impacts on composite structures. *Finite Elements in Analysis and Design* 2014; **86**:23–33.
167. Prakash A, Taciroglu E, Hjelmstad KD. Computationally efficient multi-time-step method for partitioned time integration of highly nonlinear structural dynamics. *Computers & Structures* 2014; **133**:51–63.
168. Brun M, Gravouil A, Combescure A, Limam A. Two FETI-based heterogeneous time step coupling methods for Newmark and α-schemes derived from the energy method. *Computer Methods in Applied Mechanics and Engineering* 2014. DOI: 10.1016/j.cma.2014.09.010.